Effect of soil saturation on denitrification in a grassland soil

Laura Maritza Cardenas[1*], Roland Bol, R.[2], Dominika Lewicka-Szczebak,[3], Andrew Stuart Gregory[4], Graham Peter Matthews[5], William Richard Whalley[4], Thomas Henry Misselbrook[1], David Scholefield[1] and Reinhard Well[3]

[1]Rothamsted Research, North Wyke, Okehampton, Devon EX20 2SB, United Kingdom
[2]Institute of Bio- and Geosciences, IBG-3/Agrosphere, Forschungszentrum Jülich GmbH, 52428 Jülich, Germany
[3]Thünen Institute of Climate-Smart Agriculture, Federal Research Institute for Rural Areas, Forestry and Fisheries, Bundesallee, 50, D-38116 Braunschweig, Germany
[4]Rothamsted Research, Harpenden, Hertfordshire AL5 2JQ, United Kingdom
[5]University of Plymouth, Drake Circus, Plymouth, Devon PL4 8AA, United Kingdom
**Correspondence to:* Laura M. Cardenas (laura.cardenas@rothamsted.ac.uk)

Abstract. Nitrous oxide (N_2O) is of major importance as a greenhouse gas and precursor of ozone (O_3) destruction in the stratosphere mostly produced in soils. The soil emitted N_2O is generally predominantly derived from denitrification and to a smaller extent, nitrification, both processes controlled by environmental factors and their interactions, and are influenced by agricultural management. Soil water content expressed as water filled pore space (WFPS) is a major controlling factor of emissions and its interaction with compaction, has not been studied at the micropore scale. A laboratory incubation was carried out at different saturation levels for a grassland soil and emissions of N_2O and N_2 were measured as well as the isotopocules of N_2O. We found that fluxes variability was larger in the less saturated soils probably due to nutrient distribution heterogeneity created from soil cracks and consequently nutrient hot spots. The results agreed with denitrification as the main source of fluxes at the highest saturations, but nitrification could have occurred at the lower saturation, even though moisture was still high (71% WFSP). The isotopocules data indicated isotopic similarities in the wettest treatments vs the two drier ones. The

results agreed with previous findings where it is clear there are 2 N-pools with different dynamics: added N producing intense denitrification, vs soil N resulting in less isotopic fractionation.

Keywords

Grassland, nitrous oxide, isotopologues, isotopocule, greenhouse gases

1 Introduction

Nitrous oxide (N_2O) is of major importance as a greenhouse gas and precursor of ozone (O_3) destruction in the stratosphere (Crutzen, 1970). Agriculture is a major source of greenhouse gases (GHGs), such as carbon dioxide (CO_2), methane (CH_4) and also N_2O (IPCC, 2006). The application of organic and inorganic fertiliser N to agricultural soils enhances the production of N_2O (Baggs *et al.*, 2000). This soil emitted N_2O is predominantly derived from denitrification and to a smaller extent, nitrification in soils (Davidson and Verchot, 2000). Denitrification is a microbial process in which reduction of nitrate (NO_3^-) occurs to produce N_2O, and N_2 is the final product of this process, benign for the environment, but represents a loss of N in agricultural systems. Nitrification is an oxidative process in which ammonium (NH_4^+) is converted to NO_3^- (Davidson and Verchot, 2000). Both processes are controlled by environmental factors and their interactions, and are influenced by agricultural management (Firestone and Davidson, 1989). It is well recognised that soil water content expressed as water filled pore space (WFPS) is a major controlling factor and as Davidson (1991) illustrated, nitrification is a source of N_2O until WFPS values reach about 70%, after which denitrification dominates. In fact, Firestone and Davidson (1989) gave oxygen supply a ranking of 1 in importance as a controlling factor in fertilised soils, above C and N. At WFPS between 45 and 75% a mixture of nitrification and denitrification act as N_2O sources. Davidson also suggested that at WFPS values above 90% only N_2 is produced. Several studies have later proposed models to relate WFPS with emissions (Schmidt *et al.*, 2000; Dobbie and Smith, 2001; Parton *et al.*, 2001; del Prado *et al.*, 2006; Castellano *et al.*, 2010) but the "optimum" WFPS for N_2O emissions varies from soil to soil (Davidson, 1991). Soil structure could be influencing this effect and it has been identified to strongly interact with soil moisture (Ball *et al.*, 1999; van Groenigen *et al.*, 2005) through changes in

WFPS. Particularly soil compaction due to livestock treading and the use of heavy machinery affect soil structure and emissions as reported by studies relating bulk density to fluxes (Klefoth *et al.*, 2014b); and degrees of tillage to emissions (Ludwig *et al.*, 2011).

Compaction is known to affect the size of the larger pores (macropores) thereby reducing the soil air volume and therefore increasing the WFPS (for the same moisture content) (van der Weerden *et al.*, 2012). However, little is known about the effect of compaction on the smaller soil pores (micropores) and this could provide valuable information for understanding the simultaneous behaviour of the dynamics of water in the various pore sizes in soil. Such an understanding would lead to the development of better N_2O mitigation strategies via dealing with soil compaction issues.

The role of water in soils is closely linked to microbial activity but also relates to the degree of aeration and gas diffusivity in soils (Morley and Baggs, 2010). Water facilitates nutrient supply to microbes and restricts gas diffusion, thereby increasing the residence time of gases in soil, and the chance of further N_2O reduction before it can be released to the atmosphere. This is further aided by the restriction of the diffusion of atmospheric O_2 (Dobbie and Smith, 2001), increasing the potential for denitrification. As a consequence, counteracting effects (high microbial activity vs low diffusion) occur simultaneously making it difficult to predict net processes and corresponding outputs (Davidson, 1991). Detailed understanding of the sources of N_2O and the influence of physical factors, i.e. soil structure and its interaction with moisture, is a powerful basis for developing effective mitigation strategies.

Isotopocules of N_2O represent the isotopic substitution of the O and/or the two N atoms within the N_2O molecule. The isotopomers of N_2O, are those differing in the peripheral (β) and central N-positions (α) of the linear molecule (Toyoda and Yoshida, 1999) with the intramolecular ^{15}N site preference (SP; the difference between $\delta^{15}N^{\alpha}$ - $\delta^{15}N^{\beta}$) used to identify production processes at the level of microbial species or enzymes involved (Toyoda *et al.*, 2005; Ostrom, 2011). Moreover, $\delta^{18}O$, $\delta^{15}N$ and SP of emitted N_2O depend on the denitrification product ratio (N_2O / (N_2+N_2O)), and hence provide insight into the dynamics of N_2O reduction (Well and Flessa, 2009; Lewicka-Szczebak *et al.*, 2014; Lewicka-Szczebak *et al.*, 2015). Koster *et al.* (2013) for example recently reported $\delta^{15}N^{bulk}$ values of N_2O between –36.8‰ and –31.9‰ under the conditions of their experiment, which are indicative of denitrification according to Perez *et al.* (2006) and Well and Flessa (2009) who proposed the range –54 to –10‰ relative to the substrate. Baggs (2008) summarised that values between –90 to –40‰ are indicative of nitrification. Determination of these values are normally carried out in pure culture studies or in conditions favouring either production or reduction of N_2O (Well and Flessa, 2009). The SP is however considered a better predictor of the N_2O source due to its independence from the substrate signature (Ostrom, 2011).

Simultaneous occurrence production and reduction of N_2O as in natural conditions presents a challenge for isotopic factors determination due to uncertainty on N_2 reduction and the co-existence of different microbial communities producing N_2O (Lewicka-Szczebak *et al.*, 2014). Recently, using data from the experiment reported here, where soil was incubated under aerobic atmosphere and the complete denitrification process occurs, Lewicka-Szczebak *et al.* (2015) determined fractionation factors associated with N_2O production and reduction using a modelling approach. The analysis comprised measurements of the N_2O and N_2 fluxes combined with isotopocule data. Net isotope effects (η values) are variable to a certain extent as they result from a combination of several processes causing isotopic fractionation (Well et al., 2012). The results generally confirmed the range of values of η (net isotope effects) and $\eta^{18}O/\eta^{15}N$ ratios reported by previous studies for N_2O reduction for that part of the soil volume were denitrification was enhanced by the N+C amendment. This did not apply for the other part of the soil volume not reached by the N+C amendment, showing that the validity of published net isotope effects for soil conditions with low denitrification activity still needs to be evaluated.

Lewicka-Szczebak *et al.* (2015) observed a clear relationship between ^{15}N and ^{18}O isotope effects during N_2O production and denitrification rates. For N_2O reduction, differential isotope effects were observed for two distinct soil pools characterized by different product ratios N_2O / (N_2+N_2O). For moderate product ratios (from 0.1 to 1.0) the range of isotope effects given by previous studies was confirmed and refined, whereas for very low product ratios (below 0.1) the net isotope effects were much smaller. In this paper, we present the results from the gas emissions measurements from soils collected from a long-term permanent grassland soil to assess the impact of different levels of soil saturation on N_2O and N_2 and CO_2 emissions after compaction. CO_2 emissions were measured in addition as an estimate of aerobic respiration and thus of O_2 consumption, which indicates denitrification is promoted. The measurements included the soil isotopomer ($^{15}N_{\alpha}$, $^{15}N_{\beta}$ and site preference) analysis of emitted N_2O, which in combination with the bulk ^{15}N and ^{18}O was used to distinguish between N_2O from bacterial denitrification and other processes (e.g. nitrification and fungal denitrification) (Lewicka-Szczebak, 2017).

We conducted measurements at defined saturation of pores size fractions as a prerequisite to model denitrification as a function of water status (Butterbach Bahl *et al.*, 2013 and Müller and Clough, 2014). We have under controlled conditions created a single compaction stress of 200 kPa (typical of soils compacted after grazing) in incremental layers using a uniaxial pneumatic piston to simulate a grazing pressure. We hypothesized that at high water saturation, spatial heterogeneity of N emissions decreases due to more homogeneous distribution of the soil nutrients and/or anaerobic microsites. We also hypothesized that even at high soil moisture a mixture of nitrification and denitrification can occur. We also aimed to assess how these effects (spatial heterogeneity and source processes) occur in a relatively narrow range of moisture (70-100%). As far as we know there no other studies going to this level of detail. We aimed to understand changes in the ratio $N_2O/(N_2O+N_2)$ at the different moisture levels studied in a controlled manner on soil micro and macropores. Moreover, we used isotopocule values of N_2O to evaluate if the contribution of bacterial denitrification to the total N_2O flux was affected by moisture status.

2 Materials and methods

2.1 Soil used in the study

An agricultural soil, under grassland management since at least 1838 (Barré *et al.*, 2010), was collected from a location adjacent to a long-term ley-arable experiment at Rothamsted Research in

Hertfordshire (Highfield, see soil properties in Table 1 and further details in Rothamsted Research, 2006; Gregory *et al.*, 2010). The soil had been under permanent cut mixed-species (predominantly *Lolium* and *Trifolium*) vegetation. The soil was sampled as described in Gregory *et al.* (2010). Briefly it was sampled from the upper 150 mm of the profile, air dried in the laboratory, crumbled and sieved (<4 mm), mixed to make a bulk sample and equilibrated at a pre-determined water content (37 g 100 g^{-1}; Gregory *et al.*, 2010) in air-tight containers at 4° C for at least 48 hours.

1.2.Preparation of soil blocks

The equilibrated soil was then packed into twelve stainless steel blocks (145 mm diameter; h: 100 mm), each of which contained three cylindrical holes (i.d: 50 mm; h: 100 mm each). The cores were packed to a single compaction stress of 200 kPa in incremental layers using a uniaxial pneumatic piston. The three hole- blocks were used to facilitate the compression of the cores. The 200 kPa stress was analogous to a severe compaction event by a tractor (Gregory *et al.*, 2010) or livestock (Scholefield *et al.*, 1985). The total area of the upper surface of soil in each block was therefore 58.9 cm^2 (3×19.6 cm^2) and the target volume of soil was set to be 544.28 cm^3 (3×181.43 cm^3) with the objective of leaving a headspace of approximately 45 cm^3 (3×15 cm^3) for the subsequent experiment. The precise height of the soil (and hence the volume) was measured using the displacement measurement system of a DN10 Test Frame (Davenport-Nene, Wigston, Leicester, UK) with a precision of 0.001 mm.

2.3 Equilibration of soil cores at different saturations

The soil was equilibrated to four different initial saturation conditions or treatments (t0) which were based on the likely distribution of water between macropores and micropores. The first treatment was where both the macro- and micropores (and hence the total soil) was fully saturated; the second treatment was where the macropores were half-saturated and the micropores remained fully saturated; the third treatment was where the macropores were fully unsaturated and the micropores again remained fully saturated; and the fourth treatment was where the macropores were fully unsaturated and the micropores were half-saturated. These four treatments are hereafter referred to as SAT/sat;

HALFSAT/sat; UNSAT/sat and UNSAT/halfsat, respectively, where upper-case refers to the saturation condition of the macropores and lower-case refers to the saturation condition of the micropores. In order to set these initial saturation conditions, we referred to the gravimetric soil water release characteristic for the soil, as given in Gregory *et al.* (2010) (see supplement 1). To achieve target water contents during the incubation, the amount of liquid added with the C/N amendment (15 mL) was taken into account in the total volume of water added. For the SAT/sat and HALFSAT/sat conditions, two sets of three replicate blocks were placed on two fine-grade sand tension tables connected to a water reservoir. For the UNSAT/sat condition a set of three replicate blocks was placed on a tension plate connected to a water reservoir, and the final set of three replicate blocks were placed in pressure plate chambers connected to high-pressure air. All blocks were saturated on their respective apparatus for 24 h, and were then equilibrated for 7 days at the adjusted target matric potentials which were achieved by either lowering the water level in the reservoir (sand tables and tension plate) or by increasing the air pressure (pressure chambers). At the end of equilibration period, the blocks were removed carefully from the apparatus, wrapped in air-tight film, and maintained at 4 °C until the subsequent incubation.

2.4 Incubation

The study was carried out under controlled laboratory conditions, using a specialised laboratory denitrification (DENIS) incubation system (Cardenas *et al.*, 2003). Each block containing three cores was placed in an individual incubation vessel of the automated laboratory system in a randomised block design to avoid effect of vessel. The lids for the vessels containing three holes were lined with the cores in the block to ensure that the solution to be applied later would fall on top of each soil core. Stainless steel bulkheads fitted (size for ¼” tubing) on the lids had a three-layered Teflon coated silicone septum (4 mm thick x 7 mm diameter) for supplying the amendment solution by using a gas tight hypodermic syringe. The bulkheads were covered with a stainless steel nut and only open when amendment was applied. The incubation experiment lasted 13 days. The incubation vessels with the soils were contained in a temperature controlled cabinet and the temperature set at

20°C. The incubation vessels were flushed from the bottom at a rate of 30 ml min^{-1} with a He/O_2 mixture (21% O_2, natural atmospheric concentration) for 24 h, or until the system and the soils atmosphere were emitting low background levels of both N_2 and N_2O (N_2 can get down to levels of 280 ppm much smaller than atmospheric values). Subsequently, the He/O_2 supply was reduced to 10 ml min^{-1} and directed across the soil surface and measurements of N_2O and N_2 carried out at approximately 2 hourly cycles to sample from all the 12 vessels. Emissions of CO_2 were simultaneously measured.

2.5 Application of amendment

An amendment solution equivalent to 75 kg N ha^{-1} and 400 kg C ha^{-1} was applied as a 5 ml aliquot a solution containing KNO_3 and glucose to each of the three cores in each vessel on day 0 of the incubation. Glucose is added to optimise conditions for denitrification to occur (Morley and Baggs, 2010). The aliquot was placed in a stainless steel container (volume 1.2 l) which had three holes drilled with bulkheads fitted, two to connect stainless steel tubing for flushing the vessel, and the third one to place a septum on a bulkhead to withdraw solution. Flushing was carried out with He for half an hour before the solution was required for application to the soil cores and continued during the application process to avoid atmospheric N_2 contamination (a total of one and a half hours). The amendment solution was manually withdrawn from the container with a glass syringe fitted with a three-way valve onto the soil surface; care was taken to minimise contamination from atmospheric N_2 entering the system. The syringe content was injected to the soil cores via the inlets on the lids consecutively in each lid (three cores) and all vessels, completing a total of 36 applications that lasted about 45 minutes. Incubation continued for twelve days, and the evolution of N_2O, N_2 and CO_2 was measured continuously. At the end of each incubation experiment, the soils were removed from the incubation vessels for further analysis. The three cores in each incubation vessel were pooled in one sample and subsamples taken and analysed for mineral N, total N and C and moisture status.

2.6 Gas measurements

Gas samples were directed to the relevant analysers via an automated injection valve fitted with 2 loops to direct the sample to two gas chromatographs. Emissions of N_2O and CO_2 were measured by Gas Chromatography (GC), fitted with an Electron Capture Detector (ECD) and separation achieved by a stainless steel packed column (2 m long, 4 mm bore) filled with 'Porapak Q' (80–100 mesh) and using N_2 as the carrier gas. The detection limit for N_2O was equivalent to 2.3 g N ha^{-1} d^{-1}. The N_2 was measured by GC with a He Ionisation Detection (HID) and separation achieved by a PLOT column (30 m long 0.53 mm i.d.), with He as the carrier gas. The detection limit was 9.6 g N ha^{-1} d^{-1}. The response of the two GCs was assessed by measuring a range of concentrations for N_2O, CO_2 and N_2. Parent standards of the mixtures 10133 ppm N_2O + 1015.8 ppm N_2; 501 ppm N_2O + 253 ppm N_2 and 49.5 ppm N_2O + 100.6 ppm N_2 were diluted by means of Mass Flow controllers with He to give a range of concentrations of: for N_2O of up to 750 ppm and for N_2 1015 ppm. For CO_2 a parent standard of 30,100 ppm was diluted down to 1136 ppm (all standards were in He as the balance gas). Daily calibrations were carried out for N_2O and N_2 by using the low standard and doing repeated measurements. The temperature inside the refrigeration cabinet containing the incubation vessels was logged on an hourly basis and checked at the end of the incubation. The gas outflow rates were also measured and recorded daily, and subsequently used to calculate the flux.

2.7 Measurement of N_2O isotopic signatures

Gas samples for isotopocule analysis were collected in 115 ml serum bottles sealed with grey butyl crimp-cap septa (Part No 611012, Altmann, Holzkirchen, Germany). The bottles were connected by a Teflon tube to the end of the chamber vents and were vented to the atmosphere through a needle, to maintain flow through the experimental system. Dual isotope and isotopocule signatures of N_2O, i.e. $\delta^{18}O$ of N_2O ($\delta^{18}O$-N_2O), average $\delta^{15}N$ ($\delta^{15}N^{bulk}$) and $\delta^{15}N$ from the central N-position ($\delta^{15}N^{\alpha}$) were analysed after cryo-focussing by isotope ratio mass spectrometry as described previously (Well *et al.*, 2008). ^{15}N site preference (SP) was obtained as SP = 2 * ($\delta^{15}N^{\alpha}$ – $\delta^{15}N^{bulk}$). Dual isotope and isotopocule ratios of a sample (R_{sample}) were expressed as ‰ deviation from $^{15}N/^{14}N$ and $^{18}O/^{16}O$

ratios of the reference standard materials (R_{std}), atmospheric N_2 and standard mean ocean water (SMOW), respectively:

$$\delta X = (R_{sample}/R_{std} - 1) \times 1000 \qquad [2]$$

where X = $^{15}N^{bulk}$, $^{15}N^{\alpha}$, $^{15}N^{\beta}$, or ^{18}O

2.8 Data analysis and additional measurements undertaken

The areas under the curves for the N_2O, CO_2 and N_2 data were calculated by using GenStat 11 (VSN International Ltd, Hemel Hempstead, Herts, UK). The resulting areas for the different treatments were analysed by applying analysis of variance (*ANOVA).* The isotopic ($^{15}N^{bulk}$, ^{18}O, and site preference (SP) differences between the four treatment for the different sampling dates were analysed by two-way ANOVA. We also used the Student's *t* test to check for changes in soil water content over the course of the experiments.

Calculation of the relative contribution of the N_2O derived from bacterial denitrification (%B_{DEN}) was done according to Lewicka-Szczebak *et al.* (2015). The isotopic value of initially produced N_2O, *i.e*. prior to its partial reduction (δ_0) was determined using a Rayleigh model (Mariotti *et al.*, 1982), were δ_0 is calculated using the fractionation factor of N_2O reduction ($\eta_{N2O\text{-}N2)}$ for SP and the fraction of residual N_2O (r_{N2O}) which is equal to the $N_2O/(N_2+N_2O)$ product ratio obtained from direct measurements of N_2 and N_2O flux. An endmember mixing model was then used to calculate the percentage of bacterial N_2O in the total N_2O flux (%B_{DEN}) from calculated δ_0 values and the SP and $\delta^{18}O$ endmember values of bacterial denitrification and fungal denitrification/nitrification. The range in endmember and $\eta_{N2O\text{-}N2}$ values assumed (adopted from Lewicka-Szczebak, 2017) to calculated maximum and minimum estimates of %B_{DEN} is given in Table 4.

Because both, endmember values and $\eta_{N2O\text{-}N2}$values are not constant but subject to the given ranges, we calculated here several scenarios using combinations of maximum, minimum and average endmember and $\eta_{N2O\text{-}N2}$ values (Table 4) to illustrate the possible range of %B_{DEN} for each sample. For occasional cases where %B_{DEN} > 100% the values were set to 100%.

At the same time as preparing the main soil blocks, a set of replicate samples was prepared in exactly the same manner, but in smaller cores (i.d: 50 mm; h: 25 mm). On these samples we analysed soil mineral N, total N and C and moisture at the start of the incubation. The same parameters were measured after incubation by doing destructive sampling from the cores. Mineral N (NO_3^-, NO_2^- and NH_4^+) was analysed after extraction with KCl by means of a segmented flow analyser using a colorimetric technique (Searle, 1984). Total C and N in the air dried soil were determined using a thermal conductivity detector (TCD, Carlo Erba, model NA2000). Soil moisture was determined by gravimetric analysis after drying at 105°C.

3 Results

3.1 Soil composition

The results after moisture adjustment at the start of the experiment resulted in a range of WFPS of 100 to 71% for the 4 treatments (Table 2). The results from the end of the incubation also confirmed that there remained significant differences in soil moisture between the high moisture treatments (SAT/sat and HALFSAT/sat) and the two lower moisture treatments (Table 3; one-way ANOVA, $p<0.05$). Soil in the two wettest states lost statistically significant amounts of water (10% ($p=0.006$) and 4.4% ($p<0.001$) for SAT/sat and HALFSAT/sat, respectively) over the course of the 13-day incubation experiment. This was inevitable as there was no way to hold a high (near-saturation) matric potential once the soil was inside the DENIS assembly, and water would have begun to drain by gravitational forces out of the largest macropores (>30 µm). An additional factor was the continuous He/O_2 delivery over the soil surface which would have caused some drying. We accepted these as unavoidable features of the experimental set-up, but we assume that the main response of the gaseous emissions occurred under the initial conditions, prior to the loss of water over subsequent days. Soil in the two drier conditions had no significant change in their water content over the experimental period ($p= 0.153$ and 0.051 for UNSAT/sat and UNSAT/halfsat, respectively). The results of the initial soil composition were, for mineral N: 85.5 mg NO_3^--N kg^{-1} dry soil, 136.2 mg NH_4^+-N kg^{-1} dry soil. The mineral N contents of the soils at the end of the incubation are reported in Table 3 showing that NO_3^- was very small in treatments SAT/sat and HALFSAT/sat (~1 mg N kg^{-1} dry soil) compared to UNSAT/sat and UNSAT/halfsat (50-100 mg N kg^{-1} dry soil) at the end of the incubation. Therefore, there was a significant difference in soil NO_3^- between the former, high moisture treatments and the latter drier (UNSAT) treatments which were also significantly different between themselves ($p<0.001$ for both). The NH_4^+ content was similar in treatments SAT/sat, HALFSAT/sat and UNSAT/sat (~100 mg N kg^{-1} dry soil), but slightly lower in treatment UNSAT/halfsat (71.3 mg N kg^{-1} dry soil), however overall differences were not significant probably due to the large variability on the driest treatment ($p>0.05$).

3.2 Gaseous emissions of N_2O, CO_2 and N_2

All datasets of N_2O and N_2 emissions showed normal distribution (Fpr.<0.001). The treatments SAT/sat and HALFSAT/sat for all three gases, N_2O, CO_2 and N_2 showed fluxes that were well replicated for all the vessels (see Fig. 1), in contrast for UNSAT/sat and UNSAT/halfsat the emissions between the various replicated vessel in each treatment was not as consistent, leading to a larger within treatment variability in the magnitude and shape of the GHG fluxes measured. The cumulative fluxes also resulted in larger variability for the drier treatments (Table 3).

Nitrous oxide and nitrogen gas. The general trend was that the N_2O concentrations in the headspace increased shortly after the application of the amendment (Fig. 1). The duration of the N_2O peak for each replicate soil samples was about three days, except for UNSAT/halfsat in which one of the replicate soils exhibit a peak which lasted for about 5 days. The N_2O maximum in the SAT/sat and HALFSAT/sat treatments was of similar magnitude (means of 5.5 and 6.5 kg N ha^{-1} d^{-1}, respectively) but not those of UNSAT/sat and UNSAT/halfsat (means of 7.1 and 11.9 kg N ha^{-1} d^{-1}, respectively). The N_2 concentrations always increased before the soil emitted N_2O reached the maximum. The lag between both N_2O and N_2 peak for all samples was only few hours. Peaks of N_2 generally lasted just over four days, except in UNSAT/halfsat where one replicate lasted about 6 days (Fig. 1). Unlike in the N_2O data, there was larger within treatment variability in the replicates for all four treatments. The standard deviations of each mean (Table 3) also indicate the large variability in treatments UNSAT/sat and UNSAT/halfsat for both N_2O and N_2.

The product ratios, i.e. $N_2O/(N_2O+N_2)$ resulted in a peak just after amendment addition by ca. 0.73 (at 0.49 d), 0.65 (at 0.48 d), 0.99 (at 0.35 d) and 0.88 (at 0.42 d) for SAT/sat, HALFSAT/sat, UNSAT/sat and UNSAT/halfsat, respectively, and then decreases gradually until day 3 where it becomes nearly zero for the 2 wettest treatments, and stays stable for the driest treatments between 0.1-0.2 (see Table 5 where the daily means of these ratios are presented).

The cumulative areas of the N_2O and N_2 peaks analysed by one-way ANOVA resulted in no significant differences between treatments for both N_2O and N_2 (Table 3). Due to the large variation in treatments UNSAT/sat and UNSAT/halfsat we carried out a pair wise analysis by using a weighted t-test (Cochran, 1957). This analysis resulted in treatment differences between SAT/sat and HALFSAT/sat, HALFSAT/sat and UNSAT/sat, SAT/sat and UNSAT/sat, but only at the 10% significance level ($P < 0.1$ for both N_2O and N_2).

The results showed that total N emission (N_2O+N_2) (Table 3) decreased between the highest and lowest soil moistures i.e. from 63.4 for SAT/sat (100% WFPS) to 34.1 kg N ha^{-1} (71% WFPS) for UNSAT/halfsat. The maximum cumulative N_2O occurred at around 80% WFPS (Fig. 2) whereas the total N_2O+N_2 was largest at about 95% and for N_2 it was our upper treatment at 100% WFPS.

Carbon dioxide. The background CO_2 fluxes (before amendment application, i.e. day -1 to day 0) were high at around 30 kg C ha^{-1} d^{-1} and variable (not shown). The CO_2 concentrations in the headspace increased within a few hours after amendment application. The maximum CO_2 flux was reached earlier in the drier treatments (about 1-2 days; ~70 kg C ha^{-1} d^{-1}) compared to the wettest (3 days; ~40 kg C ha^{-1} d^{-1}) and former peaks were also sharper (Fig. 1). The cumulative CO_2 fluxes were significantly larger in the two drier unsaturated treatments (ca. 400-420 kg C ha^{-1}) when compared to the wetter more saturated treatment (ca. 280-290 kg C ha^{-1}, $P<0.05$) (Table 3).

3.3 Isotopocules of N_2O

The $\delta^{15}N^{bulk}$ of the soil emitted N_2O in our study differed significantly among the four treatments and between the seven sampling dates ($p<0.001$ for both); there was also a significant treatment*sampling date interaction ($p<0.001$). The maximum $\delta^{15}N^{bulk}$ generally occurred on day 3, except for SAT/sat on day 4 (Table 6).

The maximum $\delta^{18}O$-N_2O values were also found on day 3, except for SAT/sat which peaked at day 2 (Table 6). Overall, the $\delta^{18}O$-N_2O values varied significantly between treatment and sampling dates ($p<0.001$ for both), but there was no significant treatment*time interaction ($p>0.05$).

The site preference (SP) for the SAT/sat treatment had an initial maximum value on day 2 (6.3‰) which decreased thereafter in the period from day 3 to 5 to a mean SP values of the emitted N_2O of 2.0‰ on day 5, subsequently rising to 8.4‰ on day 12 of the experiment (Table 6). The HALFSAT/sat treatment had the highest initial SP values on day 2 and 3 (both 6.4‰), decreasing again to a value of 2.0‰, but now on day 4 followed by subsequent higher SP values of up to 9.2‰ on day 7 (Table 6). The two driest treatments (UNSAT/sat and UNSAT/halfsat) both had an initial maximum on day 3 (11.9‰ and 5.9‰, respectively), and in UNSAT/sat the SP value then decreased to day 7 (3.9‰), but in UNSAT/halfsat treatment after a marginal decrease on day 4 (5.4‰) it then increased throughout the experiment reaching 11.8‰ on day 12 (Table 6). The lowest SP values were generally on day 1 in all treatments. Overall, for all parameters, there was more similarity between the more saturated treatments SAT/sat and HALFSAT/sat, and between the two more dry and aerobic treatments UNSAT/sat and UNSAT/halfsat.

The N_2O / (N_2O + N_2) ratios vs SP for all treatments in the first two days (when N_2O was increasing and the N_2O / (N_2O + N_2) ratio was decreasing) shows a significant negative response of the SP when the ratio increased (Fig. 3). This behaviour suggests that when the emitted gaseous N is dominated by N_2O (ratio close to 1) the SP values will be slightly negative with an intercept of -2‰ (Fig. 3), i.e. within the SP range of bacterial denitrification. With decreasing N_2O / (N_2O + N_2) ratio the SP values of soil emitted N_2O were increasing to values up to 8‰. This is in juxtaposition with the situation when the N emissions are dominated by N_2 or N_2O is low, where the SP values of soil emitted N_2O were much higher (Fig. 3), pointing to an overall product ratio related to an 'isotopic shift' of 10 to 12.5‰. We fitted 3 functions through this data including a second degree polynomial, a linear and logarithmic function. The fitted logarithmic function in Fig. 3, is in almost perfect agreement with Lewicka-Szczebak *et al.* (2014). Lewicka-Szczebak *et al.* (2014) data fits on the top left of Fig. 3.

It has been reported that the combination of the isotopic signatures of N_2O potentially identifies the contribution of processes other than bacterial denitrification (Köster *et al*., 2015; Wu Di *et al*., 2016; Deppe *et al*., 2017). The question arises to which extent the relationships between the $\delta^{18}O$ and δ^{15}Nbulk and between $\delta^{18}O$ and SP within the individual treatments denitrification dynamics. We checked this to evaluate the robustness of isotope effects during N_2O reduction as a prerequisite to calculate the percentage of bacterial denitrification in N_2O productionIn our data, maximum $\delta^{18}O$ and SP values, were generally observed at or near the peak of N_2 emissions on days 2-3, independent of the moisture treatment (Table 6 and Fig. 3). $\delta^{15}N^{bulk}$ values of all treatments were mostly negative when N_2O fluxes started to increase (day 1, Fig. 1, Table 6), except for UNSAT/halfsat in which the lowest value was before amendment application, reaching their highest values between days 3 and 4 for when N_2O fluxes were back to the low initial values, and then decreased during the remaining period. $\delta^{18}O$ values increased about 10 - 20‰ after day 1 reaching maximum values on days 2 or 3 in all treatments, while SP increased in parallel, at least by 3‰ (SAT/sat) and up to 12‰(UNSAT/sat). While $\delta^{18}O$ exhibited a steady decreasing trend after day 3, SP behaved opposite to $\delta^{15}N^{bulk}$ with decreasing values while $\delta^{15}N^{bulk}$ was rising again after days 4 or 5.

We further explored the data by looking at the relationships between the $\delta^{18}O$ and $\delta^{15}N^{bulk}$ for all the treatments. The $\delta^{18}O$ vs $\delta^{15}N^{bulk}$ for all treatments is presented separating the data in three periods (Fig. 4): '-1', with $\delta^{18}O$ vs $\delta^{15}N^{bulk}$ values 1 day prior to the moisture adjustment (and N and C application); '1-2', with values in the first 2 days after the addition of water, N and C were added and N_2O emissions were generally increasing in all treatments; and, '3-12', the period in days after moisture adjustment and N and C addition when N_2O emissions generally decreased back to baseline soil emissions. There was a strong and significant relationship ($P<0.001$ and 0.05, respectively) between $\delta^{18}O$ vs $\delta^{15}N^{bulk}$ for the high moisture treatments (R^2= 0.973 and 0.923 for SAT/sat and HALFSAT/sat, respectively) at the beginning of the incubation ('1-2') when the N_2O emissions are still increasing, in contrast to those of the lower soil moisture treatments that were lower and not significant (R^2= 0.294 and 0.622, for UNSAT/sat and UNSAT/halfsat, respectively). The relationships between $\delta^{18}O$ vs $\delta^{15}N^{bulk}$ of emitted N_2O for the '3-12' period were significant for SAT/sat and HALFSAT/sat with R^2 values between 0.549 and 0.896 and P values <0.05 and 0.001, respectively (Fig. 4). Regressions were also significant for this period for the driest treatments ($P<0.001$). Interestingly, with decreasing soil moisture content (Fig. 4a to 4d) the regression lines of '1-2' and '3-12' day period got closer together in the graphs. Overall, the $\delta^{15}N^{bulk}$ isotopic distances between the two lines was larger for a given $\delta^{18}O$-N_2O value for SAT/sat and HALFSAT/sat (ca. 20‰) when compared to the UNSAT/sat and UNSAT/halfsat treatments (ca. 13‰) (Fig. 4). So it seems the $\delta^{15}N^{bulk}$ / $\delta^{18}O$-N_2O signatures are more similar for the drier soils than the two wettest treatments. In addition, Fig 4 exactly reflects the 2-pool dynamics with increasing $\delta^{15}N$ and $\delta^{18}O$ while the product ratio goes down (days 2,3), then only $\delta^{15}N$ continue increasing due to fractionation of the NO_3^- during exhaustion of pool 1 in the wet soil (days 3,4,5), finally as pool 1 is depleted and more and more comes from pool 2, the product ratio increases somewhat, and $\delta^{15}N$ decreases somewhat since pool 2 is less fractionated and also $\delta^{18}O$ decreases due to slightly increasing product ratio. Note that the turning points of $\delta^{18}O$ and product ratio (Table 3 and 4) for the wetter soils almost coincide.

Similarly to Fig. 4, $\delta^{18}O$ vs the SP (Fig. 5) was analysed for the different phases of the experiment. Generally, the slopes (Table 7) for days 1-2 for the three wettest treatments were similar (~0.2-0.3) following the range of known reduction slopes and also had high and significant ($P<0.05$) regression coefficients (R^2= 0.65, 0.90 and 0.87 for SAT/sat, HALFSAT/Sat and UNSAT/sat, respectively). The slopes on days 3-5 were variable but slightly similar on days 7-12 (between 41 and 0.68) for the same three treatments. They were only significant for the 2 driest treatments ($P<0.05$). On days 7-12 SAT/sat and UNSAT/sat gave significant correlations ($P<0.001$ and 0.05, respectively). Figure 5 also shows the "map" for the values of SP and $\delta^{18}O$ from all treatments. Reduction lines (vectors) represent minimum and maximum routes of isotopocules values with increasing N_2O reduction to N_2 based on the reported range in the ratio between the isotope fractionation factors of N_2O reduction for SP and $\delta^{18}O$ (Lewicka-Szczebak et al., (2017). Most samples are located within the vectors (from Lewicka-Szczebak *et al.* 2017) area of N_2O production by bacterial denitrification with partial N_2O reduction to N_2 (within uppermost and lowermost N_2O reduction vectors representing the extreme values for the bacterial endmember and reduction slopes). Only a few values of the UNSAT/sat and UNSAT/halfsat treatments are located above that vector area and more close or within the vector area of mixing between bacterial denitrification and fungal denitrification/nitrification.

The estimated ranges of the proportion of emitted N_2O resulting from bacterial denitrification ($\%B_{DEN}$) were on day 1 and 2 after the amendment comparable in all four moisture treatments (Table 6). However, during day 3 to 12 the $\%B_{DEN}$ ranged from 78-100% in SAT/sat and 79-100% HALFSAT/Sat, which was generally higher than that estimated at 54-86% for UNSAT/halfsat treatment. The $\%B_{DEN}$ of the UNSAT/halfsat in that period was intermediate between SAT/sat and UNSAT/sat with range of range 60-100% (Table 6). The final values were similar to those on day -1 except for the UNSAT/sat treatment.

4 Discussion

4.1 N_2O and N_2 fluxes

The observed decrease in total N emissions with decreasing initial soil moisture reflects the effect of soil moisture as reported in previous studies (Well *et al.*, 2006). The differences when comparing the cumulative fluxes however, were only marginally ($p<0.1$) significant (Table 3) mostly due to large variability within replicates in the drier treatments (see Fig. 1b). Davidson *et al.* (1991) provided a

WFPS threshold for determination of source process, with a value of 60% WFPS as the borderline between nitrification and denitrification as source processes for N_2O production. The WFPS in all treatments in our study was larger than 70%, above this 60% threshold, and referred to as the "optimum water content" for N_2O by Scheer *et al.* (2009), so we can be confident that denitrification was likely to have been the main source process in our experiment. In addition, Bateman *et al.* (2004) observed the largest N_2O fluxes at 70% WFPS on a silty loam soil, lower than the 80% value for the largest fluxes from the clay soil in our study (Fig. 2) suggesting that this optimum value could change with soil type. Further, the maximum total measured N lost (N_2O+N_2) in our study occurred at about 95% WFPS (Fig. 2), but not many studies report N_2 fluxes for comparison and we are still missing measurements of nitric oxide (NO) (Davidson *et al.*, 2000) and ammonia (NH_3) to account for the total N losses. It is however possible that the N_2O+N_2 fluxes in the SAT/sat treatment were underestimated due to low diffusivity in the water filled pores (Well *et al.*, 2001). Gases would have been trapped (particularly in the higher saturation treatments) due to low diffusion and thus possibly masked differences in N_2 and N_2O production since this fraction of gases was not detected (Harter et al. 2016). It is worth mentioning that there was some drying during the incubation. The flow of the gas is very slow (10 ml/min) simulating a low wind speed so normally this would dry the soil in field conditions too. It would represent a rainfall event where the initial moisture differs between treatments but some drying occurs due to the wind flow. We believe however, that the effect of drying will be more relevant (and significant relative to the initial moisture) later in the incubation.

The smaller standard errors in both N_2O and N_2 data for the larger soil moisture levels (Table 3 and Fig. 1) could suggest that at high moisture contents nutrient distribution (N and C) on the top of the core is more homogeneous making replicate cores to behave similarly. At the lower soil moisture for both N_2O and N_2, it is possible that some cracks appear on the soil surface causing downwards nutrient movement, resulting in heterogeneity in nutrient distribution on the surface and increasing variability between replicates, reflected in the larger standard errors of the fluxes. Laudone *et al.* (2011) studied, using a biophysical model, the positioning of the hot-spot zones away from the critical percolation path (described as ‘where air first breaks through the structure as water is removed at increasing tensions’) and found it slowed the increase and decline in emission of CO_2, N_2O and N_2. They found that hot-spot zones further away from the critical percolation path would reach the anaerobic conditions required for denitrification in shorter time, the products of the denitrification reactions take longer to migrate from the hot-spot zones to the critical percolation path and to reach the surface of the system. The model and its parameters can be used for modelling the effect of soil compaction and saturation on the emission of N_2O. They suggest that having determined biophysical parameters influencing N_2O production, it remains to determine whether soil structure, or simply saturation, is the determining factor when the biological parameters are constrained. Furthermore, Clough *et al.* (2013) indicate that microbial scale models need to be included on larger models linking microbial processes and nutrient cycling in order to consider spatial and temporal variation. Kulkarni *et al.* (2008) refers to “hot spots” and “hot moments” of denitrification as scale dependant and highlight the limitations for extrapolating fluxes to larger scales due to these inherent variabilities.

Well *et al.* (2003) found that under saturated conditions there was good agreement between laboratory and field measurements of denitrification, and attributed deviations, under unsaturated conditions, to spatial variability of anaerobic microsites and redox potential. Dealing with spatial variability when measuring N_2O fluxes in the field remains a challenge, but the uncertainty could be potentially reduced if water distribution is known. Our laboratory study suggests that soil N_2O and N_2 emission for higher moisture levels would be less variable than for drier soils and suggests that for the former a smaller number of spatially defined samples will be needed to get an accurate field estimate. This applied to a lesser extent to the CO_2 fluxes.

Our results, for the two highest water contents (SAT/sat and HALFSAT/sat), indicated that N_2O only contributed 20% of the total N emissions, as compared to 40-50% at the lowest water contents (UNSAT/sat and UNSAT/halfsat, Table 3). This was due to reduction to N_2 at the high moisture level, confirmed by the larger N_2 fluxes, favoured by low gas diffusion which increased the N_2O residence time and the chance of further transformation (Klefoth *et al.*, 2014a). We should also consider the potential underestimation of the fluxes in the highest saturation treatment due to restricted diffusion in the water filled pores (Well *et al.*, 2001). A total of 99% of the soil NO_3^- was consumed in the two high water treatments, whereas in the drier UNSAT/sat and UNSAT/halfsat treatments there still was 35% and 70% of the initial amount of NO_3^- left in the soil, at the end of the incubation, respectively (Table 3). The total amount of gas lost compared to the NO_3^- consumed was almost 3 times for the wetter treatments, and less than twice for the 2 drier ones. This agrees with denitrification as the dominant process source for N_2O with larger consumption of NO_3^- at the higher moisture and larger N_2 to N_2O ratios (5.7, 4.7 for SAT/sat and HALFSAT/sat, respectively), whereas at the lower moisture, ratios were lower (1.5 and 1.0 for UNSAT/sat and UNSAT/halfsat, respectively) (Davidson, 1991). This also indicates that with WFPS above the 60% threshold for N_2O production from denitrification, there was an increasing proportion of anaerobic microsites with increase in saturation controlling NO_3^- consumption and N_2/N_2O ratios in an almost linear manner. With WFPS values between 71-100 % and N_2/N_2O between 1.0 and 5.7, a regression can be estimated: $Y=0.1723\ X - 11.82$ ($R^2=0.8585$), where Y is N_2/N_2O and X is %WFPS. In summary, we propose that heterogeneous distribution of anaerobic microsites could have been the limiting factor for complete depletion of NO_3^- and conversion to N_2O in the two drier treatments. In addition, in the UNSAT/halfsat treatment there was a decrease in soil NH_4^+ at the end of the incubation (almost 50%; Table 3) suggesting nitrification could have been occurring at this water content which also agrees with the increase in NO_3^-, even though WFPS was relatively high (>71%) (Table 3). It is important to note that as we did not assess gross nitrification, the observed net nitrification based on lowering in NH_4^+ could underestimate gross nitrification since there might have been substantial N mineralisation during the incubation. However, under conditions favouring denitrification at high soil moisture the typical N_2O produced from nitrification is much lower compared to that from denitrification (Lewicka-Szczebak *et al.*, 2017) with the maximum reported values for the N_2O yield of nitrification of 1-3 % (e.g. Deppe *et al*., 2017). If this is the case, nitrification fluxes could not have exceeded 1 kg N with NH_4^+ loss of < 30 kg * 3% ~1 kg N. This would have represented for the driest treatment, if conditions were suitable only for one day, that nitrification-derived N_2O would have been 6% of the total N_2O produced. Loss of NH_3 was not probable at such low pH (5.6). The corresponding rate of NO_3^- production using the initial and final soil contents and assuming other processes were less important in magnitude, would have been < 1 mg NO_3^--N kg dry soil^{-1} d^{-1} which is a reasonable rate (Hatch *et al.*, 2002). The other three treatments lost similar amounts of soil NH_4^+ during the incubation (23-26%) which could have been due to some degree of nitrification at the start of the incubation before O_2 was depleted in the soil microsites or due to NH_4^+ immobilisation (Table 3) (Geisseler *et al.*, 2010).

A mass N balance, taking into account the initial and final soil NO_3^-, NH_4^+, added NO_3^- and the emitted N (as N_2O and N_2) results in unaccounted N-loss of 177.2, 177.6, 130.6 and 110.8 mg N kg^{-1} for SAT/sat, HALFSAT/sat, UNSAT/sat and UNSAT/halfsat, respectively, that could have been emitted as other N gases (such as NO), and some, immobilised in the microbial biomass. NO fluxes reported by Loick et al. (2016) for example, result in a ratio N_2O/NO of 0.4. In summary unaccounted-for N loss is two to three times the total measured gas loss (Table 3). In addition, in the SAT/sat treatment there was probably an underestimation of the produced N_2 and N_2O due to restricted diffusion at the high WFPS (e.g. Well *et al.*, 2001).

4.2 Isotopocule trends.

Trends of isotopocule values of emitted N_2O coincided with those of N_2 and N_2O fluxes. The results from the isotopocule data (Table 6 and Fig. 3) also indicated that generally there were more isotopic similarities between the two wettest treatments when compared to the two contrasting drier soil moisture treatments.

Isotopocule values of emitted N_2O reflect multiple processes where all signatures are affected by the admixture of several microbial processes, the extent of N_2O reduction to N_2 as well as the variability of the associated isotope effects (Lewicka-Szczebak *et al.*, 2015). Moreover, for $\delta^{18}O$ and $\delta^{15}N^{bulk}$ the precursor signatures are variable (Decock and Six, 2013), for $\delta^{18}O$ the O exchange with water can be also variable (Lewicka-Szczebak *et al.*, 2017). Since the number of influencing factors clearly exceeds the number of isotopocule values, unequivocal results can only be obtained if certain processes can be excluded or be determined independently, (Lewicka-Szczebak *et al.*, 2015; Lewicka-Szczebak, 2017). The two latter conditions were fulfilled in this study, i.e. N_2O fluxes were high and several order of magnitude above possible nitrification fluxes, since the N_2O – to- NO_3^- ratio yield of nitrification products rarely exceeds 1% (Well *et al.*, 2008; Zhu et al., 2012). Moreover, N_2 fluxes and thus N_2O reduction rates were exactly quantified.

The estimated values of % B_{DEN} indicate that in the period immediately after amendment application all moisture treatments were similar, reflecting that the microbial response to N and C added was the same and denitrification dominated. This was the same for the rest of the period for the wetter treatments. In the drier treatments, proportions decreased afterwards and were similar to values before amendment application, possibly due to recovery of more aerobic conditions that could have encouraged other processes to contribute. As N_2 was still produced in the driest treatment, (but in smaller amounts), this indicated ongoing denitrifying conditions and thus large contributions to the total N_2O flux from nitrification were not probable, but some occurred as suggested by NH_4^+ consumption.

The trends observed reflect the dynamics resulting from the simultaneous application of NO_3^- and labile C (glucose) on the soil surface as described in previous studies (Meijide *et al.*, 2010; Bergstermann *et al.*, 2011) where the same soil was used, resulting in two locally distinct NO_3^- pools with differing denitrification dynamics. In the soil volume reached by the NO_3^-/glucose amendment, denitrification was initially intense with high N_2 and N_2O fluxes and rapid isotopic enrichment of the NO_3^--N. When the NO_3^- and/or glucose of this first pool were exhausted, N_2 and N_2O fluxes were much lower and dominated by the initial NO_3^- pool that was not reached by the glucose/NO_3^- amendment and that is less fractionated due to its lower exhaustion by denitrification, causing decreasing trends in $\delta^{15}N^{bulk}$ of emitted N_2O.

This is also reflected in Fig 4 where N_2O fluxes from both pools exhibited correlations (and mostly significant) between $\delta^{15}N^{bulk}$ and $\delta^{18}O$ due to varying N_2O reduction, but $\delta^{15}N^{bulk}$ values in days 1 and 2 - i.e. the phase when Pool 1 dominated - were distinct from the previous and later phase.

The fit of $^{15}N^{bulk}$ /^{18}O data to two distinct and distant regression lines can be attributed to two facts: Firstly, in the wet treatment (Fig 4a, b) Pool 1 was probably completely exhausted and there was little NO_3^- formation from nitrification (indicated by final NO_3^- values close to 0, Table 3) whereas the drier treatment exhibited substantial NO_3^- formation and high residual NO_3^-. Hence, there was probably still some N_2O from Pool 1 after day 2 in the dry treatment but not in the wetter ones. Secondly, the product ratios after day 2 of the drier treatments were higher (0.13 to 0.44) compared to the wetter treatments (0.001 to 0.09). Thus the isotope effect of N_2O reduction was smaller in the drier treatments, leading to a smaller upshift of $\delta^{15}N^{bulk}$ and thus more negative values after day 2, i.e. with values closer to days 1 +2.

This finding further confirms that $\delta^{15}N/\delta^{18}O$ patterns are useful to identify the presence of several N pools, e.g. typically occurring after application of liquid organic fertilizers which has been previously demonstrated using isotopocule patterns (Koster *et al.*, 2015).

Interestingly, the highest $\delta^{15}N^{bulk}$ and $\delta^{18}O$ values of the emitted N_2O were found in the soils of the HALFSAT/sat treatment, although it may have been expected that the highest isotope values from the N_2O would be found in the wettest soil (SAT/sat) because N_2O reduction to N_2 is favoured under water-saturated conditions due to extended residence time of produced N_2O (Well et al., 2012). However, $N_2O/(N_2+N_2O)$ ratios of the SAT/sat and SAT/halfsat treatments were not different (Table 5). Bol *et al.* (2004) also found that some estuarine soils under flooded conditions (akin to our SAT/sat) showed some strong simultaneous depletions (rather than enrichments) of the emitted N_2O $\delta^{15}N^{bulk}$ and $\delta^{18}O$ values. These authors suggested that this observation may have resulted from a flux contribution of an 'isotopically' unidentified N_2O production pathway. Another explanation could be complete consumption of some of the produced N_2O in isolated micro-niches in the SAT/sat treatment due to inhibited diffusivity in the fully saturated pores space. N_2 formation in these isolated domains would not affect the isotopocule values of emitted N_2O and this would thus result in lower apparent isotope effects of N_2O reduction in water saturated environments as suggested by Well *et al.* (2012).

The SP values obtained were generally below 12‰ in agreement with reported ranges attributed to bacterial denitrification: -2.5 to 1.8‰ (Sutka *et al.*, 2006); 3.1 to 8.9‰ (Well and Flessa, 2009); -12.5 to 17.6‰ (Ostrom, 2011). The SP, believed to be a better predictor of the N_2O source as it is independent of the substrate isotopic signature (Ostrom, 2011), has been suggested as it can be used to estimate N_2O reduction to N_2 in cases when bacterial denitrification can be assumed to dominate N_2O fluxes (Koster *et al.*, 2013; Lewicka-Szczebak *et al.*, 2015). There was a strong correlation between the SP and N_2O / (N_2O+N_2) ratios on the first 2 days of the incubation for all treatments up until the N_2O reached its maximum (Fig. 3) which reflects the accumulation of $\delta^{15}N$ at the alpha position during ongoing N_2O reduction to N_2. Later on in the experiment beyond day 3, this was not observed probably because in that period the product ratio remained almost unchanged and very low (Table 6). Similar observations have been reported by Meijide *et al.* (2010) and Bergstermann *et al.* (2011), as they also found a decrease in SP during the peak flux period in total N_2+N_2O emissions, but only when the soil had been kept wet prior to the start of the experiment (Bergstermann *et al.*, 2011). These results confirm from 2 independent studies (Lewicka-Szczebak *et al.*, 2014) that there is a relationship between the product ratios and isotopic signatures of the N_2O emitted. The $\delta^{18}O$ vs SP regressions indicate more similarity between the three wettest treatments as well as high regression coefficients, suggesting this SP/$\delta^{18}O$ ratio could also be used to help identify patterns for emissions and their sources.

4.3 Link to modelling approaches.

Since isotopocule data could be compared to N_2 and N_2O fluxes, the variability of isotope effects of N_2O production and reduction to N_2 by denitrification could be determined from this data set (Lewicka-Szczebak *et al.*, 2015) and this included modelling the two pool dynamics discussed above. It was demonstrated that net isotope effects of N_2O reduction ($\eta_{N2O\text{-}N2}$) determined for both NO_3^- pools differed. Pool 1 representing amended soil and resulting in high fluxes but moderate product ratio, exhibited η_{N2O-N2} values and the characteristic $\eta^{18}O/\eta^{15}N$ ratios similar to those previously reported, whereas for Pool 2 characterized by lower fluxes and very low product ratio, the net isotope effects were much smaller and the $\eta^{18}O/\eta^{15}N$ ratios, previously accepted as typical for N_2O reduction processes (i.e., higher than 2), were not valid. The question arises, if the poor coincidence of Pool 2 isotopologue fluxes with previous N_2O reduction studies reflects the variability of isotope effects of N_2O reduction or if the contribution of other processes like fungal denitrification could explain this (Lewicka-Szczabak *et al.*, 2017). The latter explanation is evaluated in section 4.3

Liu *et al.* (2016) noted that on the catchment scale potential N_2O emission rates were related to hydroxylamine and NO_3^-, but not NH_4^+ content in soil. Zou *et al.* (2014) found high SP (15.0 to 20.1‰) values at WFPS of 73 to 89% suggesting that fungal denitrification and bacterial nitrification contributed to N_2O production to a degree equivalent to that of bacterial denitrification.

To verify the contribution of fungal denitrification and/or hydroxylamine oxidation we can first look at the $\eta SP_{N2O-NO3}$ values calculated in the previous modelling study applied on the same dataset, (Table 1, the final modelling Step, Lewicka-Szczebak *et al.*, 2015). For Pool 1 there are no significant differences between the values of various treatments, SP_0 ranges from (-1.8±4.9) to (+0.1±2.5). Pool 1 emission was mostly active in days 1-2, hence these values confirm the bacterial dominance in the emission at the beginning of incubation, which originates mainly from the amendment addition and represent similar pathway for all treatments. However, for the Pool 2 emission we could observe a significant difference when compared the two wet treatments (SAT/sat and HALFSAT/sat: (-5.6±7.0)) with the UNSAT/sat treatment (+3.8±5.8). This represents the emission from unamended soil which was dominating after the third day of the incubation and indicates higher nitrification contribution for the drier treatment.

4.4 Contribution of bacterial denitrification.

An endmember mixing approach has been previously used to estimate the fraction of bacterial N_2O ($\%B_{DEN}$), but without independent estimates of N_2O reduction (Zou *et al.*, 2014), but due to the unknown isotopic shift by N_2O reduction, the ranges of minimum and maximum estimates were large, showing that limited information is obtained without N_2 flux measurement.

In an incubation study with two arable soils, Koster *et al.* (2013) used $N_2O/(N_2+N_2O)$ ratios and isotopocule values of gaseous fluxes to calculate SP of N_2O production (referred to as SP_0), which is equivalent to SP_0 using the Rayleigh model and published values of $\eta_{N2O\text{-}N2}$. The endmember mixing approach based on SP_0 was then used to estimate fungal denitrification and/or hydroxylamine oxidation giving indications for a substantial contribution in a clay soil, but not in a loamy soil. Here we presented for the first time an extensive data set with large range in product ratios and moisture to calculate the contribution of bacterial denitrification ($\%B_{DEN}$) of emitted N_2O from SP_0. The uncertainty of this approach arises from three factors, (i) from the range of SP_0 endmember values for bacterial denitrification of -11 to 0 per mil and 30 to 37 for hydroxylamine oxidation/fungal denitrification, (ii) from the range of net isotope effect values of N_2O reduction ($\eta_{N2O\text{-}N2}$) for SP which vary from -2 to -8 per mil (Lewicka-Szczebak *et al.*, 2015), and iii) system condition (open vs. closed) taken to estimate the net isotope effect (Wu *et al.*, 2016).

The observation that $\%B_{DEN}$ of emitted N_2O was generally high (63-100%) in the wettest treatment (SAT/sat) was not unexpected. However interestingly $\%B_{DEN}$ in the HALFSAT/sat treatment was very similar (71-98%), pointing to the role of the wetter areas of the soil microaggregates contributing to high $\%B_{DEN}$ values. The slightly lower values, i.e. down 60% in UNSAT/sat $\%B_{DEN}$ range of 60-100%, suggest that the majority of N_2O derived from bacterial denitrification still results from the wetter microaggregates of the soils, despite the fact that the macropores are now more aerobic. Only, when the micropores become partially wet, as in the UNSAT/halfsat treatment, do the more aerobic soil conditions allow a higher contribution of nitrification/fungal denitrification ranging from 0 - 46% (1 - % B_{DEN}, Table 6) on days 3-12 (Zhu *et al.*, 2013). Differences in the contribution of nitrification/fungal denitrification between the flux phases when different NO_3^- pools were presumably dominating are only indicated in the driest treatment, since 1-$\%B_{DEN}$ was higher after day 2 (14 to 46%) compared to days 1+2 (0 to 33 %).

This larger share of nitrification/fungal denitrification can be attributed to the increasing contribution from Pool 2 to the total flux as indicated by the modeling of higher SP_0 for Pool 2 (see previous section and Lewicka-Szczebak *et al.* (2015). In addition, indication for elevated contribution of processes other than bacterial denitrification were only evident in the drier treatments during phases before and after N_2, N_2O fluxes were strongly enhanced by glucose amendment. The data supply no clue whether the other processes were suppressed during the anoxia induced by glucose decomposition or just masked by the vast glucose-induced bacterial N_2O fluxes.

5 Conclusions

The results from this study demonstrated that at high soil moisture levels, there was less variability in N fluxes between replicates, potentially decreasing the importance of soil hot spots in emissions at these moisture levels. At high moisture there also was complete depletion of nitrate confirming denitrification as the main pathway for N_2O emissions, and due to less diffusion of the produced N_2O, the potential for further reduction to N_2 increased. Under less saturation, but still relatively high soil moisture, nitrification occurred. Isotopic similarities were observed between similar saturation levels and patterns of $\delta^{15}N/\delta^{18}O$ and $SP/\delta^{18}O$ are suggested as indicators of source processes.

Acknowledgments

The authors would like to thank the technical help from Mark Butler during the laboratory incubation and Andrew Bristow and Patricia Butler for carrying out soil analysis. Also thanks to Dan Dhanoa for advice on statistical analysis, and to Anette Giesemann and Martina Heuer for help in N_2O isotopic analyses. This study was funded by the UK Biotechnology and Biological Sciences Research Council (BBSRC) with competitive grants BB/E001580/1 and BB/E001793/1. Rothamsted Research is sponsored by the BBSRC.

Figures

Figure 1. Mean of the three replicates for N_2O, N_2 and CO_2 emissions from a. SAT/sat treatment; b. HALFSAT/sat; c. UNSAT/sat; d. UNSAT/halfsat. Grey lines correspond to the standard error of the means.

Figure 2 Total N emissions (N_2O+N_2)-N, N_2O and N_2 vs WFPS. Fitted functions through each dataset are also shown.

Figure 3 Ratio N_2O / (N_2O + N_2) vs. Site Preference (SP) for all for treatments in the first two days. A logarithmic function was fitted through the data, the corresponding equation and correlation coefficient are given.

Figure 4 $\delta^{18}O$ vs $\delta^{15}N_{bulk}$ in all treatments for three periods (day -1 in diamond symbol, days 1-2 in square symbol and days 3-12 in triangle symbol, respectively) in the experiment: a. SAT/sat treatment; b. HALFSAT/sat; c. UNSAT/sat; d. UNSAT/halfsat. Equations of fitted functions and correlation coefficients are shown. Correlations are unadjusted, the P value tests if the slope is different from zero.

Figure 5 Site Preference vs $\delta^{18}O$ in all treatments for three periods (day -1, days 1-2 and days 3-12) in the experiment: a. SAT/sat treatment; b. HALFSAT/sat; c. UNSAT/sat; d. UNSAT/halfsat. Equations of fitted functions and correlation coefficients are in Table 7 for 1-2, 3-5 and 7-12 (5-12 for c.). Endmember areas for nitrification, N; bacterial denitrification, D; fungal denitrification, FD and nitrifier denitrification, ND and corresponding vectors or reduction lines (black solid lines) are from Lewicka-Szczebak et al., (2017), and represent minimum and maximum routes of isotopocule values with increasing N_2O reduction to N_2 based on the reported range in the ratio between the isotope fractionation factors of N_2O reduction for SP and $\delta^{18}O$ (Lewicka-Szczebak et al., 2017).

Tables

Table 1 Soil properties of the soil used in the experiment

Table 2 The four saturation conditions used for the soil in the experiment

Table 3 Contents of soil moisture, NO_3^-, NH_4^+ and C:N ratio and cumulative fluxes of N_2O and N_2 and CO_2 from all treatments at the end of the incubation.

Table 4 Scenarios with different combinations of $\delta^{18}O$ and SP endmember values and $\eta N_2O\text{-}N_2$ values to calculate maximum and minimum estimates of $\%B_{DEN}$ (minimum, maximum and average values adopted from Lewicka-Szczebak *et al.,* (2016).

Table 5 Ratios N_2O / (N_2O + N_2) for all treatments

Table 6 The temporal trends in $\delta^{15}N_{bulk}$, $\delta^{18}O$, $\delta^{15}N_{\alpha}$, SP and $\%B_{DEN}$ for all experimental treatments

Table 7 Equations of fitted functions and correlation coefficients corresponding to Figure 5 for Site Preference vs $\delta^{18}O$ in all treatments for three periods.

References

Baggs, E.M., 2008. A review of stable isotope techniques for N_2O source partitioning in soils: recent progress, remaining challenges and future considerations. Rapid Commun. Mass Sp., 22, 1664-1672.

Baggs, E.M., Rees, R.M., Smith, K.A., Vinten, A.J.A., 2000. Nitrous oxide emission from soils after incorporating crop residues. Soil Use Manage., 16, 82-87.

Ball, B.C., Scott, A., Parker, J.P., 1999. Field N_2O, CO_2 and CH_4 fluxes in relation to tillage, compaction and soil quality in Scotland. Soil Till. Res., 53, 29-39.

Barré, P., Eglin, T., Christensen, B.T., Ciais, P., Houot, S., Kätterer, T., van Oort, F., Peylin, P., Poulton, P.R., Romanenkov, V., Chenu, C., 2010. Quantifying and isolating stable soil organic carbon using long-term bare fallow experiments. Biogeosciences, 7, 3839-3850.

Bateman, E., Cadisch, G., Baggs, E., 2004. Soil water content as a factor that controls N_2O production by denitrification and autotrophic and heterotrophic nitrification. Controlling nitrogen flows and losses.12th Nitrogen Workshop, University of Exeter, UK, 21-24 September 2003, 290-292.

Bergstermann, A., Cardenas, L., Bol, R., Gilliam, L., Goulding, K., Meijide, A., Scholefield, D., Vallejo, A., Well, R., 2011. Effect of antecedent soil moisture conditions on emissions and isotopologue distribution of N_2O during denitrification. Soil Biol. Biochem., 43, 240-250.

Bol, R., Rockmann, T., Blackwell, M., Yamulki, S., 2004. Influence of flooding on delta N-15, delta O-18, (1)delta N-15 and (2)delta N-15 signatures of N_2O released from estuarine soils - a laboratory experiment using tidal flooding chambers. Rapid Commun. Mass Sp., 18, 1561-1568.

Butterbach-Bahl, K., Baggs, E. M., Dannenmann, M., Kiese, R., Zechmeister-Boltenstern, S. 2013. Nitrous oxide emissions from soils: how well do we understand the processes and their controls? Phil Trans R Soc B., 368: 20130122, http://dx.doi.org/10.1098/rstb.2013.0122.

Cardenas, L.M., Hawkins, J.M.B., Chadwick, D., Scholefield, D., 2003. Biogenic gas emissions from soils measured using a new automated laboratory incubation system. Soil Biol. Biochem., 35, 867-870.

Cardenas, L.M., Thorman, R., Ashleee, N., Butler, M., Chadwick, D., Chambers, B., Cuttle, S., Donovan, N., Kingston, H., Lane, S., Dhanoa, M.S., Scholefield, D., 2010. Quantifying annual N_2O emission fluxes from grazed grassland under a range of inorganic fertiliser nitrogen inputs. Agr. Ecosyst. Environ., 136, 218-226.

Castellano, M.J., Schmidt, J.P., Kaye, J.P., Walker, C., Graham, C.B., Lin, H., Dell, C.J., 2010. Hydrological and biogeochemical controls on the timing and magnitude of nitrous oxide flux across an agricultural landscape. Global Change Biol., 16, 2711-2720.

Clough, T.J., Muller, C., Laughlin, R.J., 2013. Using stable isotopes to follow excreta N dynamics and N_2O emissions in animal production systems. Animal : an international journal of animal bioscience, 7 Suppl 2, 418-426.

Cochran, W.G.and Cox, G.M., 1957. Experimental Design. John Wiley & Sons New York.

Crutzen, P.J., 1970. Influence of Nitrogen Oxides on Atmospheric Ozone Content. Quarterly Journal of the Royal Meteorological Society, 96, 320.

Davidson, E.A., 1991. Fluxes of nitrous oxide and nitric oxide from terrestrial ecosystems. In: Microbial production and consumption of greenhouse gases: Methane, nitrogen oxides and halomethanes. J.E. Rogers and W.B. Whitman (eds.). American Society for Microbiology, Washington, D.C., pp. 219-235.

Davidson, E.A., Hart, S.C., Shanks, C.A., Firestone, M.K., 1991. Measuring Gross Nitrogen Mineralization, Immobilization, and Nitrification by N-15 Isotopic Pool Dilution in Intact Soil Cores. J. Soil Sci., 42, 335-349.

Davidson, E.A., Keller, M., Erickson, H.E., Verchot, L.V., Veldkamp, E., 2000. Testing a conceptual model of soil emissions of nitrous and nitric oxides. Bioscience, 50, 667-680.

Davidson, E.A., Verchot, L.V., 2000. Testing the hole-in-the-pipe model of nitric and nitrous oxide emissions from soils using the TRAGNET database. Global Biogeochem. Cy., 14, 1035-1043.

Decock, C., Six, J., 2013. On the potential of delta O-18 and delta N-15 to assess N_2O reduction to N_2 in soil. Eur. J. Soil Sci., 64, 610-620.

del Prado, A., Merino, P., Estavillo, J.M., Pinto, M., Gonzalez-Murua, C., 2006. N_2O and NO emissions from different N sources and under a range of soil water contents. Nutr. Cycl. Agroecosys., 74, 229-243.

Deppe, M., Well, R., Giesemann, A., Spott, O., Flessa, H. 2017. Soil N_2O fluxes and related processes in laboratory incubations simulating ammonium fertilizer depots. Soil Biol. Biochem., 104, 68-80.

Dobbie, K.E., Smith, K.A., 2001. The effects of temperature, water-filled pore space and land use on N_2O emissions from an imperfectly drained gleysol. Eur. J. Soil Sci., 52, 667-673.

Firestone, M.K., Davidson, E.A., 1989. Microbiological basis of NO and N_2O production and consumption in soil. Exchange of Trace Gases between Terrestrial Ecosystems and the Atmosphere, 47, 7-21.

Geisseler, D., Horwath, W.R., Joergensen, R.G., Ludwig, B., 2010. Pathways of nitrogen utilization by soil microorganisms - A review. Soil Biol. Biochem., 42, 2058-2067.

Gregory, A.S., Bird, N.R.A., Whalley, W.R., Matthews, G.P., Young, I.M., 2010. Deformation and Shrinkage Effects on the Soil Water Release Characteristic. Soil Sci. Soc. Am. J., 74, 4.

Harter, J., Guzman-Bustamente, I., Kuehfuss, S., Ruser, R., Well, R., Spott, O., Kappler, A., Behrens, S. 2016. Gas entrapment and microbial N_2O reduction reduce N_2O emissions from a biochar-amended sandy clay loam soil. Scientific Reports, 6.

Hatch, D.J., Sprosen, M.S., Jarvis, S.C., Ledgard, S.F., 2002. Use of labelled nitrogen to measure gross and net rates of mineralization and microbial activity in permanent pastures following fertilizer applications at different time intervals. Rapid Commun. Mass Sp., 16, 2172-2178.

IPCC, 2006. 2006 IPCC Guidelines for National Greenhouse Gas Inventories. 2006 IPCC Guidelines for National Greenhouse Gas Inventories, Prepared by the National Greenhouse Gas Inventories Programme, Eggleston H.S., Buendia L., Miwa K., Ngara T. and Tanabe K. (eds). Published: IGES, Japan.

Klefoth, R.R., Clough, T.J., Oenema, O., Groenigen, J.W., 2014a. Soil bulk density and moisture content influence relative gas diffusivity and the reduction of nitrogen-15 nitrous oxide. Vadose Zone J., 13, 0089-0089.

Klefoth, R.R., Clough, T.J., Oenema, O., Van Groenigen, J.-W., 2014b. Soil Bulk Density and Moisture Content Influence Relative Gas Diffusivity and the Reduction of Nitrogen-15 Nitrous Oxide. Vadose Zone J., 13.

Koster, J.R., Cardenas, L.M., Bol, R., Lewicka-Szczebak, D., Senbayram, M., Well, R., Giesemann, A., Dittert, K., 2015. Anaerobic digestates lower N_2O emissions compared to cattle slurry by affecting rate and product stoichiometry of denitrification - An N_2O isotopomer case study. Soil Biol. Biochem., 84, 65-74.

Koster, J.R., Well, R., Dittert, K., Giesemann, A., Lewicka-Szczebak, D., Muhling, K.H., Herrmann, A., Lammel, J., Senbayram, M., 2013. Soil denitrification potential and its influence on N_2O reduction and N_2O isotopomer ratios. Rapid Commun. Mass Sp., 27, 2363-2373.

Kulkarni, M.V., Groffman, P.M., Yavitt, J.B., 2008. Solving the global nitrogen problem: it's a gas! Frontiers in Ecology and the Environment, 6, 199-206.

Laudone, G.M., Matthews, G.P., Bird, N.R.A., Whalley, W.R., Cardenas, L.M., Gregory, A.S., 2011. A model to predict the effects of soil structure on denitrification and N_2O emission. J. Hydrol., 409, 283-290.

Lewicka-Szczebak, D., Augustin J., Giesemann A., Well R., 2017. Quantifying N_2O reduction to N_2 based on N_2O isotopocules - validation with independent methods (Helium incubation and ^{15}N gas flux method). Biogeosciences, 14, 711-732..

Lewicka-Szczebak, D., Dyckmans, J., Kaiser, J., Marca, A., Augustin, J., Well, R., 2016. Oxygen isotope fractionation during N_2O production by soil denitrification. Biogeosciences, 13, 1129-1144.

Lewicka-Szczebak, D., Well, R., Bol, R., Gregory, A.S., Matthews, G.P., Misselbrook, T., Whalley, W.R., Cardenas, L.M., 2015. Isotope fractionation factors controlling isotopocule signatures of soil-

emitted N_2O produced by denitrification processes of various rates. Rapid Commun. Mass Sp., 29, 269-282.
Lewicka-Szczebak, D., Well, R., Koster, J.R., Fuss, R., Senbayram, M., Dittert, K., Flessa, H., 2014. Experimental determinations of isotopic fractionation factors associated with N_2O production and reduction during denitrification in soils. Geochim. Cosmochim. Ac., 134, 55-73.
Liu, S.R., Herbst, M., Bol, R., Gottselig, N., Putz, T., Weymann, D., Wiekenkamp, I., Vereecken, H., Bruggemann, N., 2016. The contribution of hydroxylamine content to spatial variability of N_2O formation in soil of a Norway spruce forest. Geochim. Cosmochim. Ac., 178, 76-86.
Loick, N., Dixon, L., Abalos, D., Vallejo, A., Matthews, G.P., McGeough, K.L., Well, R., Watson, C.J., Laughlin, R.J., Cardenas, L.M., 2016. Denitrification as a Source of Nitric Oxide Emissions from a UK Grassland Soil. Soil Biol. Biochem., 95, 1-7.
Ludwig, B., Bergstermann, A., Priesack, E., Flessa, H., 2011. Modelling of crop yields and N_2O emissions from silty arable soils with differing tillage in two long-term experiments. Soil Till. Res., 112, 114-121.
Mariotti, A., Germon, J.C., Leclerc, A., 1982. Nitrogen isotope fractionation associated with the NO-2-- N_2O step of denitrification in soils. Canadian J. Soil Sci., 62, 227-241.
Meijide, A., Cardenas, L.M., Bol, R., Bergstermann, A., Goulding, K., Well, R., Vallejo, A., Scholefield, D., 2010. Dual isotope and isotopomer measurements for the understanding of N_2O production and consumption during denitrification in an arable soil. Eur. J. Soil Sci., 61, 364-374.
Morley, N., Baggs, E.M., 2010. Carbon and oxygen controls on N_2O and N_2 production during nitrate reduction. Soil Biol. Biochem., 42, 1864-1871.
Mualem, Y., 1976. New model for predicting hydraulic conductivity of unsaturated porous-media. Water Resour. Res., 12, 513-522.
Muller, C. and Clough, T. J. 2014. Advances in understanding nitrogen flows and transformations: gaps and research pathways. J. Agric. Sci., 152: S34-S44.
Ostrom, N., Ostrom, P. , 2011. The isotopomers of nitrous oxide: analytical considerations and application to resolution of microbial production pathways. In: Baskaran M (ed). Handbook Environ Isot Geochem. Springer: Berlin Heidelberg, 453–476.
Parton, W.J., Holland, E.A., Del Grosso, S.J., Hartman, M.D., Martin, R.E., Mosier, A.R., Ojima, D.S., Schimel, D.S., 2001. Generalized model for NOx and N_2O emissions from soils. J.Geophys. Res-Atmos., 106, 17403-17419.
Perez, T., Garcia-Montiel, D., Trumbore, S., Tyler, S., De Camargo, P., Moreira, M., Piccolo, M., Cerri, C., 2006. Nitrous oxide nitrification and denitrification N-15 enrichment factors from Amazon forest soils. Ecol. Appl., 16, 2153-2167.
Scheer, C., Wassmann, R., Butterbach-Bahl, K., Lamers, J.P.A., Martius, C., 2009. The relationship between N_2O, NO, and N_2 fluxes from fertilized and irrigated dryland soils of the Aral Sea Basin, Uzbekistan. Plant Soil, 314, 273-283.
Schmidt, U., Thoni, H., Kaupenjohann, M., 2000. Using a boundary line approach to analyze N_2O flux data from agricultural soils. Nutr. Cycl. Agroecosys., 57, 119-129.
Scholefield, D., Patto, P.M., Hall, D.M., 1985. Laboratory Research on the Compressibility of 4 Topsoils from Grassland. Soil Till. Res., 6, 1-16.
Searle, P.L., 1984. The Berthelot or Indophenol Reaction and Its Use in the Analytical-Chemistry of Nitrogen - a Review. Analyst, 109, 549-568.
Sutka, R.L., Ostrom, N.E., Ostrom, P.H., Breznak, J.A., Gandhi, H., Pitt, A.J., Li, F., 2006. Distinguishing nitrous oxide production from nitrification and denitrification on the basis of isotopomer abundances. Appl. Environ. Microb., 72, 638-644.
Toyoda, S., Mutobe, H., Yamagishi, H., Yoshida, N., Tanji, Y., 2005. Fractionation of N_2O isotopomers during production by denitrifier. Soil Biol. Biochem., 37, 1535-1545.
Toyoda, S., Yoshida, N., 1999. Determination of nitrogen isotopomers of nitrous oxide on a modified isotope ratio mass spectrometer. Anal. Chem., 71, 4711-4718.
van der Weerden, T.J., Kelliher, F.M., de Klein, C.A.M., 2012. Influence of pore size distribution and soil water content on nitrous oxide emissions. Soil Research, 50, 125-135.

van Genuchten, M.T., 1980. A closed form equation for predicting the hydraulic conductivity of unsaturated soils. Soil Sci. Soc. Am. J., 44, 892-898.
van Groenigen, J.W., Kuikman, P.J., de Groot, W.J.M., Velthof, G.L., 2005. Nitrous oxide emission from urine-treated soil as influenced by urine composition and soil physical conditions. Soil Biol. Biochem., 37, 463-473.
Well, R., Augustin, J., Davis, J., Griffith, S.M., Meyer, K., Myrold, D.D., 2001. Production and transport of denitrification gases in shallow ground water. Nutr. Cycl. Agroecosys., 60, 65-75.
Well, R., Augustin, J., Meyer, K., Myrold, D.D., 2003. Comparison of field and laboratory measurement of denitrification and N_2O production in the saturated zone of hydromorphic soils. Soil Biol. Biochem., 35, 783-799.
Well, R., Eschenbach, W., Flessa, H., von der Heide, C., Weymann, D., 2012. Are dual isotope and isotopomer ratios of N_2O useful indicators for N_2O turnover during denitrification in nitrate-contaminated aquifers? Geochim. Cosmochim. Ac., 90, 265-282.
Well, R., Flessa, H., 2009. Isotopologue signatures of N_2O produced by denitrification in soils. J.Geophys. Res-Biogeo., 114.
Well, R., Flessa, H., Xing, L., Ju, X.T., Romheld, V., 2008. Isotopologue ratios of N_2O emitted from microcosms with NH_4^+ fertilized arable soils under conditions favoring nitrification. Soil Biol. Biochem., 40, 2416-2426.
Well, R., Kurganova, I., de Gerenyu, V.L., Flessa, H., 2006. Isotopomer signatures of soil-emitted N_2O under different moisture conditions - A microcosm study with arable loess soil. Soil Biol. Biochem., 38, 2923-2933.
Wu, D., Koster, J.R., Cardenas, L.M., Bruggemann, N., Lewicka-Szczebak, D., Bol, R., 2016. N_2O source partitioning in soils using N-15 site preference values corrected for the N_2O reduction effect. Rapid Commun. Mass Sp., 30, 620-626.
Wu, D., Senbayram, M., Well, R., Brüggemann, N., Pfeiffer, B., Loick, N., Stempfhuber, B., Dittert, K., Bol, R. (2017) Nitrification inhibitors mitigate N_2O emissions more effectively under straw-induced conditions favoring denitrification. Soil Biol. Biochem., 104, 197-207.
Zhu, X., Burger, M., Doane, T.A., Horwath, W.R., 2013. Ammonia oxidation pathways and nitrifier denitrification are significant sources of N_2O and NO under low oxygen availability. P. Natl. Acad. Sci. USA., 110, 6328-6333.
Zou, Y., Hirono, Y., Yanai, Y., Hattori, S., Toyoda, S., Yoshida, N., 2014. Isotopomer analysis of nitrous oxide accumulated in soil cultivated with tea (Camellia sinensis) in Shizuoka, central Japan. Soil Biol. Biochem., 77, 276-291.

Table 1. Highfield soil properties

Property	Units	Highfield
Location		Rothamsted Research
		Herts.
Grid reference	GB National Grid	TL129130
	Longitude	00°21'48"W
	Latitude	51°48'18"N
Soil type	SSEW[a] group[c]	Paleo-argillic brown earth
	SSEW[a] series[d]	Batcombe
	FAO[bc]	Chromic Luvisol
Landuse		Grass; unfertilised; cut
pH		5.63
Sand (2000-63 µm)	$g\ g^{-1}$ dry soil	0.179
Silt (63-2 µm)	$g\ g^{-1}$ dry soil	0.487
Clay (<2 µm)	$g\ g^{-1}$ dry soil	0.333
Texture	SSEW[a] class[c]	Silty clay loam
Particle density	$g\ cm^{-3}$	2.436
Organic matter	$g\ g^{-1}$ dry soil	0.089
Water content for packing	$g\ g^{-1}$ dry soil	0.37

[a]Soil Survey of England and Wales classification system
[b]United Nations Food and Agriculture Organisation World Reference Base for Soil Resources classification system (approximation)
[c]Avery (1980)
[d]Clayden & Hollis (1984)

Table 2. The four saturation conditions set for the Highfield soil.

Saturation condition	SAT/sat	HALFSAT/sat	UNSAT/sat	UNSAT/halfsat
Macropores	Saturated	Half-saturated	Unsaturated	Unsaturated
Micropores	Saturated	Saturated	Saturated	Half-saturated
As prepared:				
Matric potential, -kPa	4.1	12.3	27.3	136.9
Water content, g 100 g^{-1}	47.7	42.5	37.2	29.4
Water content, cm^{-3} 100 cm^{-3}	61.1	54.4	47.7	37.3
Water-filled pore space, %	98	91	82	68
Threshold pore size saturated, µm	73	24	11	2
Final, following amendment:				
Matric potential, -kPa	0	8.6	20.0	78.1
Water content, g 100 g^{-1}	49.8	44.6	39.3	31.5
Water content, cm^{-3} 100 cm^{-3}	63.8	57.1	50.4	40.0
Water-filled pore space, %	100	94	85	71
Threshold pore size saturated, µm	all	35	15	4

Table 3. Contents of soil moisture, NO_3^-, NH_4^+ and C:N ratio and cumulative fluxes of N_2O and N_2 and CO_2 from all treatments at the end of the incubation. Values in brackets are standard deviation of the mean of three values (emissions are expressed per area and soil weight basis).

Treatment	% Mean moisture	NO_3^-, mg N kg^{-1} dry soil	NH_4^+, mg N kg^{-1} dry soil	Total C, %	Total N, %	N_2O, kg N ha^{-1}	N_2O, mg N kg^{-1} dry soil	N_2, kg N ha^{-1}	N_2, mg N kg^{-1} dry soil	Total emitted N, kg N ha^{-1}	CO_2, kg C ha^{-1}
SAT/sat	39.8 (1.3)	1.1 (0.4)	104.3 (1.1)	3.61 (0.04)	0.35 (0.004)	9.4 (1.1)	7.8 (0.9)	54.0 (14.0)	44.8 (11.6)	63.4	289.2 (30.4)
HALFSAT/sat	40.2 (0.2)	0.8 (1.0)	104.2 (6.8)	3.64 (0.08)	0.36 (0.004)	10.9 (0.4)	9.0 (0.3)	51.7 (9.0)	42.8 (7.4)	62.6	283.0 (35.5)
UNSAT/sat	36.5 (2.1)	51.2 (37.4)	100.8 (5.7)	3.64 (0.10)	0.36 (0.007)	23.7 (11.0)	20.0 (9.5)	36.0 (28.5)	30.2 (23.7)	59.7	417.6 (57.1)
UNSAT/halfsat	34.3 (1.1)	100.6 (16.1)	71.3 (33.6)	3.53 (0.08)	0.36 (0.01)	16.8 (15.8)	14.0 (13.1)	17.2 (19.4)	14.3 (16.1)	34.1	399.7 (40.6)

Table 4: Scenarios with different combinations of $d^{18}O$ and Site Preference (SP) endmember values and η_{N2O-N2} values to calculate maximum and minimum estimates of %Bden (minimum, maximum and average values adopted from Lewicka-Szczabak et al., 2017).

	SP0BD	SP0FDN	ηSP	$\eta^{18}O$
model (min endmember plus η)	-11	30	-2	-12
model (max endmember plus η)	0	37	-8	-12
model (max endmember)	0	37	-5.4	-12
model (min endmember)	-11	30	-5.4	-12
model (max η)	-5	33	-8	-12
model (min η)	-5	33	-2	-12

Table 5. Ratios N_2O / (N_2O + N_2) for all treatments

	SAT/sat		**HALFSAT/sat**		**UNSAT/halfsat**		**UNSAT/sat**	
Days	mean	s.e.	mean	s.e.	mean	s.e.	mean	s.e.
-1	0.276	0.043	0.222	0.009	0.849	0.043	0.408	0.076
0	0.630	0.022	0.538	0.038	0.763	0.053	0.861	0.043
1	0.371	0.025	0.360	0.019	0.622	0.018	0.644	0.031
2	0.096	0.016	0.139	0.015	0.425	0.005	0.296	0.020
3	0.004	0.002	0.015	0.006	0.439	0.052	0.256	0.025
4	0.017	0.002	0.008	0.001	0.475	0.049	0.232	0.012
5	0.019	0.003	0.012	0.001	0.503	0.037	0.174	0.010
6	0.068	0.008	0.020	0.001	0.459	0.052	0.135	0.010
7	0.085	0.008	0.047	0.003	0.333	0.057	0.127	0.003
8	0.106	0.004	0.066	0.002	0.277	0.006	0.122	0.002
9	0.089	0.003	0.053	0.005	0.265	0.006	0.122	0.005
10	0.060	0.003	0.090	0.014	0.428	0.086	0.118	0.006
11	0.063	0.002	0.053	0.002	0.414	0.051	0.125	0.005

Table 6. The temporal trends in $\delta^{15}N_{bulk}$, $\delta^{18}O$, $\delta^{15}N_{\alpha}$, Site Preference (SP) and $\%B_{DEN}$ for all experimental treatments (values in brackets are the standard deviation of the mean)

	$\delta^{15}N_{bulkAIR}$ (‰)			
Day	SAT/sat	HALFSAT/sat	UNSAT/sat	UNSAT/halfsat
-1	-3.8 (2.1)	-6.2 (1.5)	-14.2 (10.9)	-23.6 (1.1)
1	-18.9 (1.6)	-25.5 (4.6)	-20.3 (2.6)	-20.8 (2.3)
2	-7.7 (4.2)	-12.7 (2.7)	-12.2 (2.0)	-13.9 (5.7)
3	-2.4 (1.8)	14.0 (2.2)	-1.1 (7.6)	-4.4 (3.0)
4	-0.9 (2.2)	-0.3 (3.6)	-7.8 (4.6)	-9.3 (3.7)
5	-6.9 (0.9)	-4.3 (6.1)	-11.3 (3.7)	-8.9 (7.7)
7	-9.6 (1.5)	-10.0 (1.6)	-14.3 (4.7)	-13.4 (13.5)
12	-7.5 (1.2)	-8.6 (0.9)	-11.8 (2.6)	-21.3 (6.9)
	$\delta^{18}O_{SMOW}$ (‰)			
	SAT/sat	HALFSAT/sat	UNSAT/sat	UNSAT/halfsat
-1	33.3 (2.6)	32.7 (3.0)	31.4 (9.8)	25.2 (4.9)
1	42.9 (2.4)	37.1 (3.8)	32.3 (3.6)	33.3 (2.1)
2	54.0 (5.7)	48.7 (4.5)	42.7 (5.3)	40.5 (5.0)
3	45.7 (1.5)	59.7 (3.2)	53.4 (5.7)	41.2 (1.0)
4	42.5 (1.4)	42.0 (3.7)	38.1 (4.5)	39.9 (7.7)
5	36.0 (2.9)	34.6 (3.7)	30.4 (2.6)	36.5 (6.9)
7	32.2 (5.5)	31.6 (5.5)	28.4 (4.4)	32.7 (5.4)
12	34.9 (5.6)	34.1 (2.7)	32.4 (2.9)	28.5 (5.0)
	$\delta^{15}N\alpha_{AIR}$ (‰)			
	SAT/sat	HALFSAT/sat	UNSAT/sat	UNSAT/halfsat
-1	-0.3 (3.4)	-2.6 (1.8)	-9.5 (12.0)	-19.7 (2.1)
1	-17.4 (1.8)	-24.0 (5.8)	-20.2 (2.0)	-21.1 (2.6)
2	-4.6 (4.2)	-9.5 (3.6)	-11.1 (1.1)	-13.8 (5.9)
3	-0.8 (1.3)	17.2 (4.0)	7.6 (4.7)	-2.7 (3.2)
4	1.0 (2.5)	0.7 (2.2)	-3.5 (3.7)	-2.8 (7.7)
5	-5.9 (0.7)	-2.9 (5.4)	-9.4 (3.9)	-5.2 (7.9)
7	-7.8 (2.3)	-5.3 (4.2)	-12.3 (5.6)	-7.7 (11.5)
12	-3.3 (2.1)	-4.6 (0.6)	-8.1 (4.2)	-15.3 (5.5)
	SP_{AIR}			
	SAT/sat	HALFSAT/sat	UNSAT/sat	UNSAT/halfsat
-1	7.0 (3.9)	7.1 (4.2)	9.4 (2.1)	7.7 (1.9)
1	2.9 (0.6)	3.0 (2.3)	0.1 (1.8)	-0.7 (1.4)
2	6.3 (0.64)	6.4 (1.9)	2.2 (2.0)	0.2 (1.9)
3	3.3 (1.0)	6.4 (6.9)	11.9 (12.4)	5.9 (0.8)
4	3.7 (0.6)	2.0 (6.2)	8.7 (5.9)	5.4 (3.0)
5	2.0 (0.4)	3.0 (2.1)	3.9 (0.5)	7.4 (2.3)
7	5.0 (2.1)	9.2 (5.2)	3.9 (1.8)	11.2 (4.1)
12	8.4 (3.3)	7.9 (0.8)	7.3 (3.7)	11.8 (5.3)
	Estimated range of $\%B_{DEN}$			
	SAT/sat	HALFSAT/sat	UNSAT/sat	UNSAT/halfsat
-1	63-100	60-100	53-85	56-84
1-2	68-100	67-100	73-100	77-100
3-12	78-100	79-100	60-100	54-86

Table 7. Equations of fitted functions and correlation coefficients corresponding to Figure 5 for Site Preference (SP) (Y axis) vs $\delta^{18}O$ (X axis) in all treatments for three periods. Correlations are unadjusted, the P value tests if the slope is different from zero.

Treatment	Days 1-2	Days 3-5	Days 7-12
SAT/sat	$y = 0.2151x - 5.8386$, $R^2 = 0.6529$ $P=0.05$	$y = 0.1204x - 1.848$, $R^2 = 0.397$ $P=0.129$	$y = 0.5872x - 12.223$, $R^2 = 0.985$ $P<0.001$
HALFSAT/sat	$y = 0.3447x - 10.129$, $R^2 = 0.9048$ $P=0.004$	$y = 0.18x - 4.5966$, $R^2 = 0.1728$ $P=0.266$	$y = 0.4063x - 6.2632$, $R^2 = 0.6876$ $P=0.171$
UNSAT/sat	$y = 0.2709x - 8.9968$, $R^2 = 0.8664$ $P=0.007$	$y = 0.7248x - 18.874$, $R^2 = 0.507$ $P=0.031$	$y = 0.6848x - 15.236$, $R^2 = 0.7156$ $P=0.034$
UNSAT/halfsat	$y = -0.0146x + 0.2506$, $R^2 = 0.0024$ $P=0.927$	$y = 0.3589x - 7.2194$, $R^2 = 0.4839$ $P=0.037$	$y = -0.318x + 21.261$, $R^2 = 0.1491$ $P=0.450$

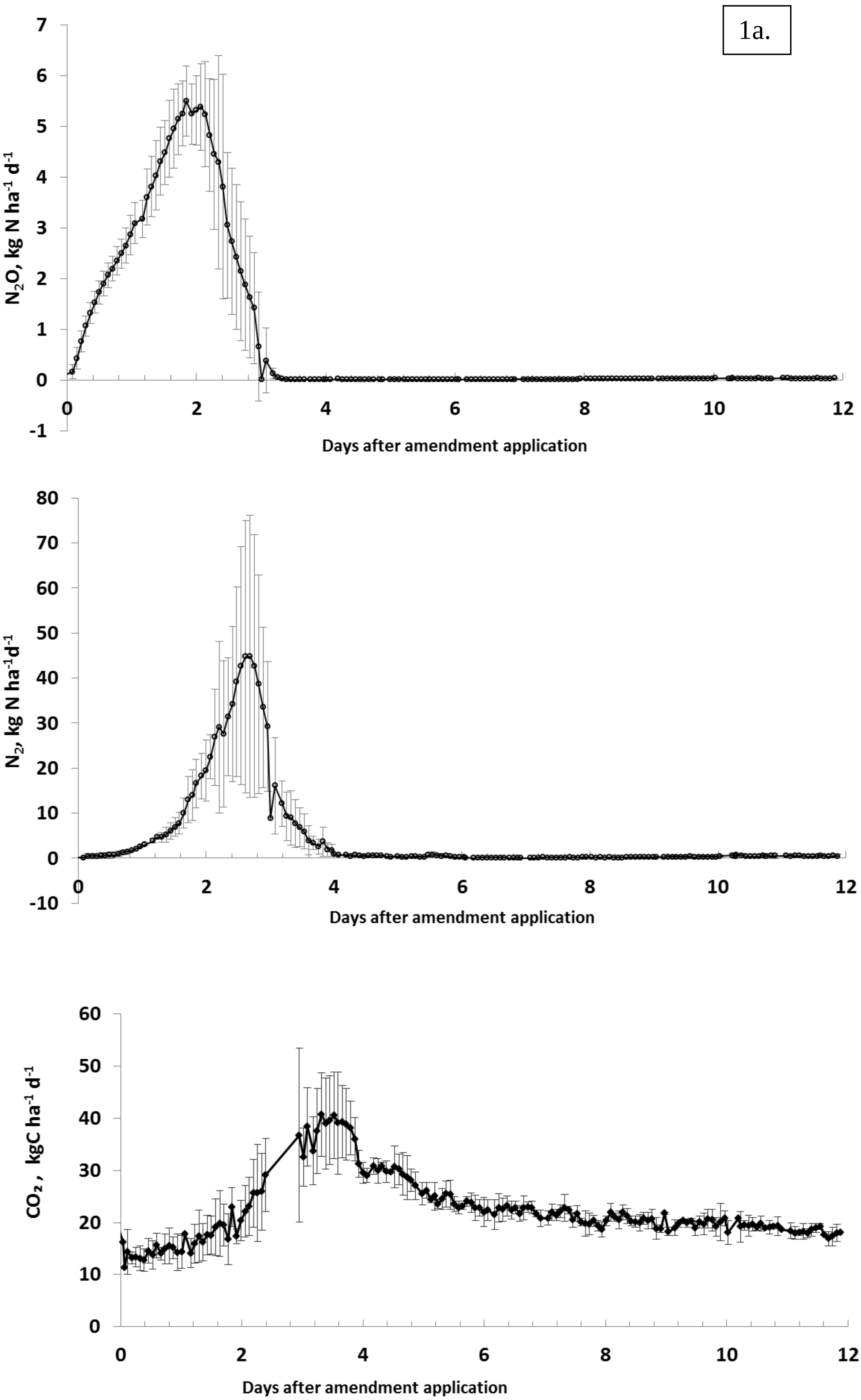
1a.
N2O, kg N ha-1 d-1
Days after amendment application
N2, kg N ha-1d-1
Days after amendment application
CO2 , kgC ha-1 d-1
Days after amendment application

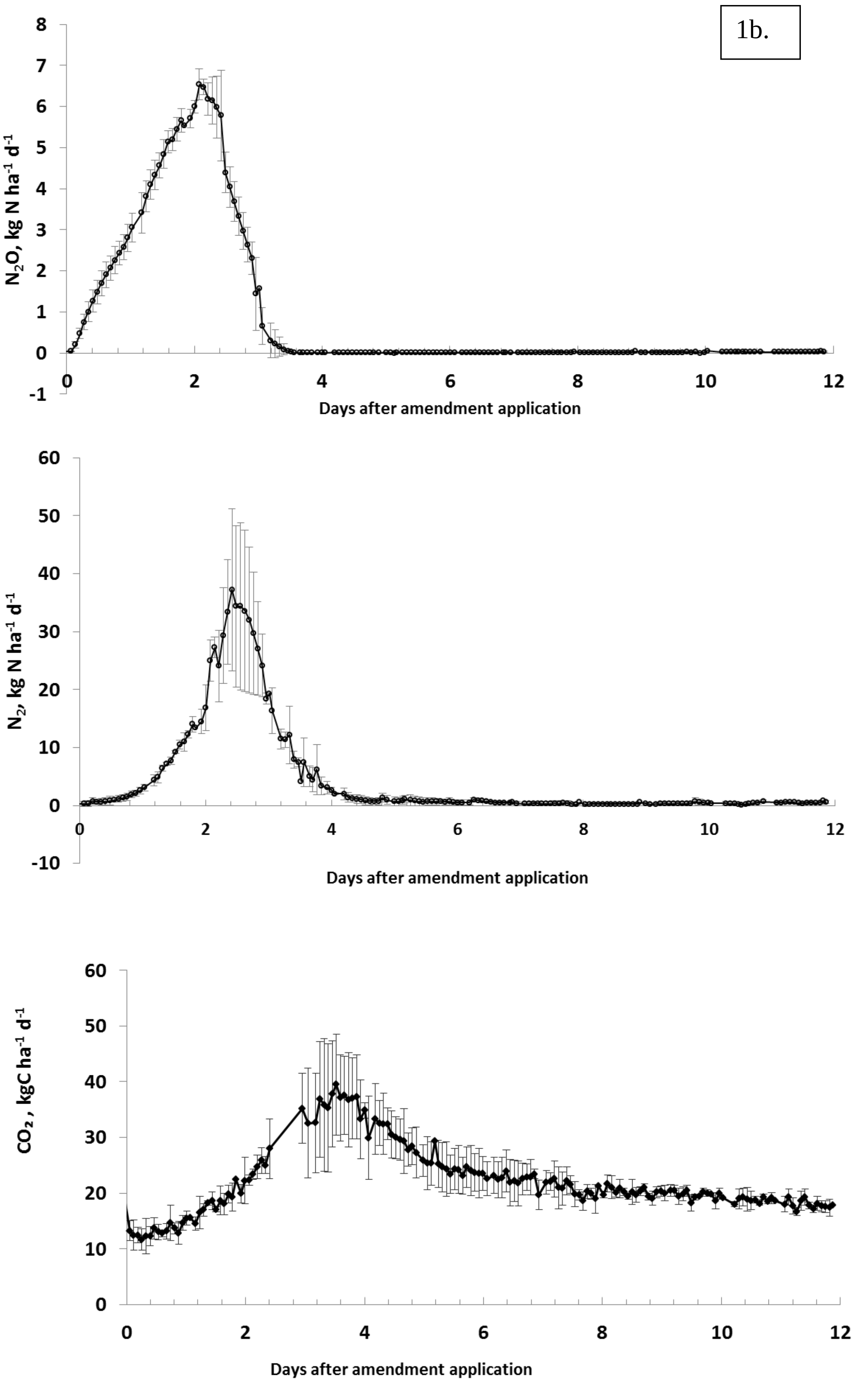
1b.
N_2O, kg N ha^{-1} d^{-1}
Days after amendment application
N_2, kg N ha^{-1} d^{-1}
Days after amendment application
CO_2 , kgC ha^{-1} d^{-1}
Days after amendment application

981

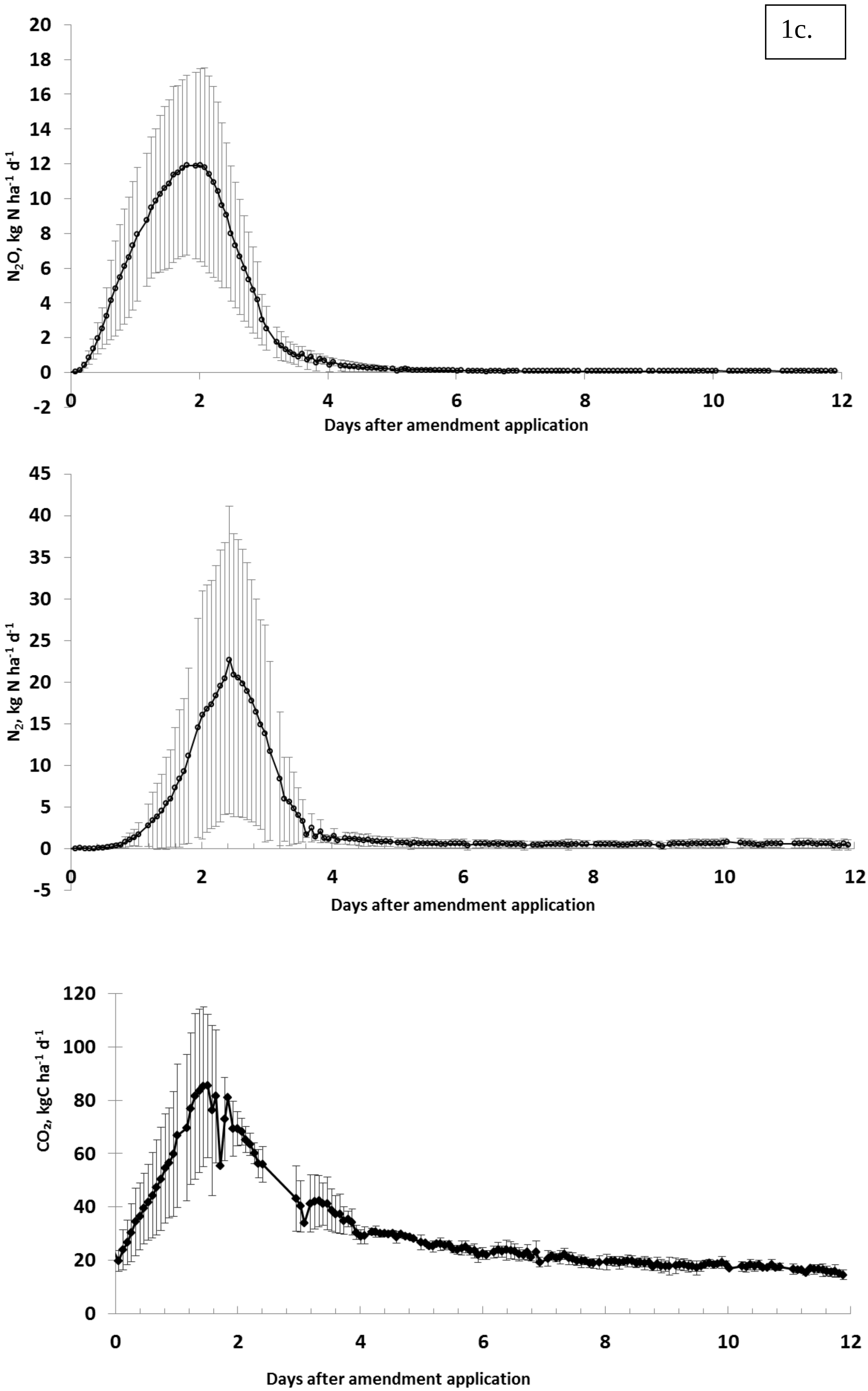
1c.
N_2O, kg N ha^{-1} d^{-1}
Days after amendment application
N_2, kg N ha^{-1} d^{-1}
Days after amendment application
CO_2, kgC ha^{-1} d^{-1}
Days after amendment application

982

1d.

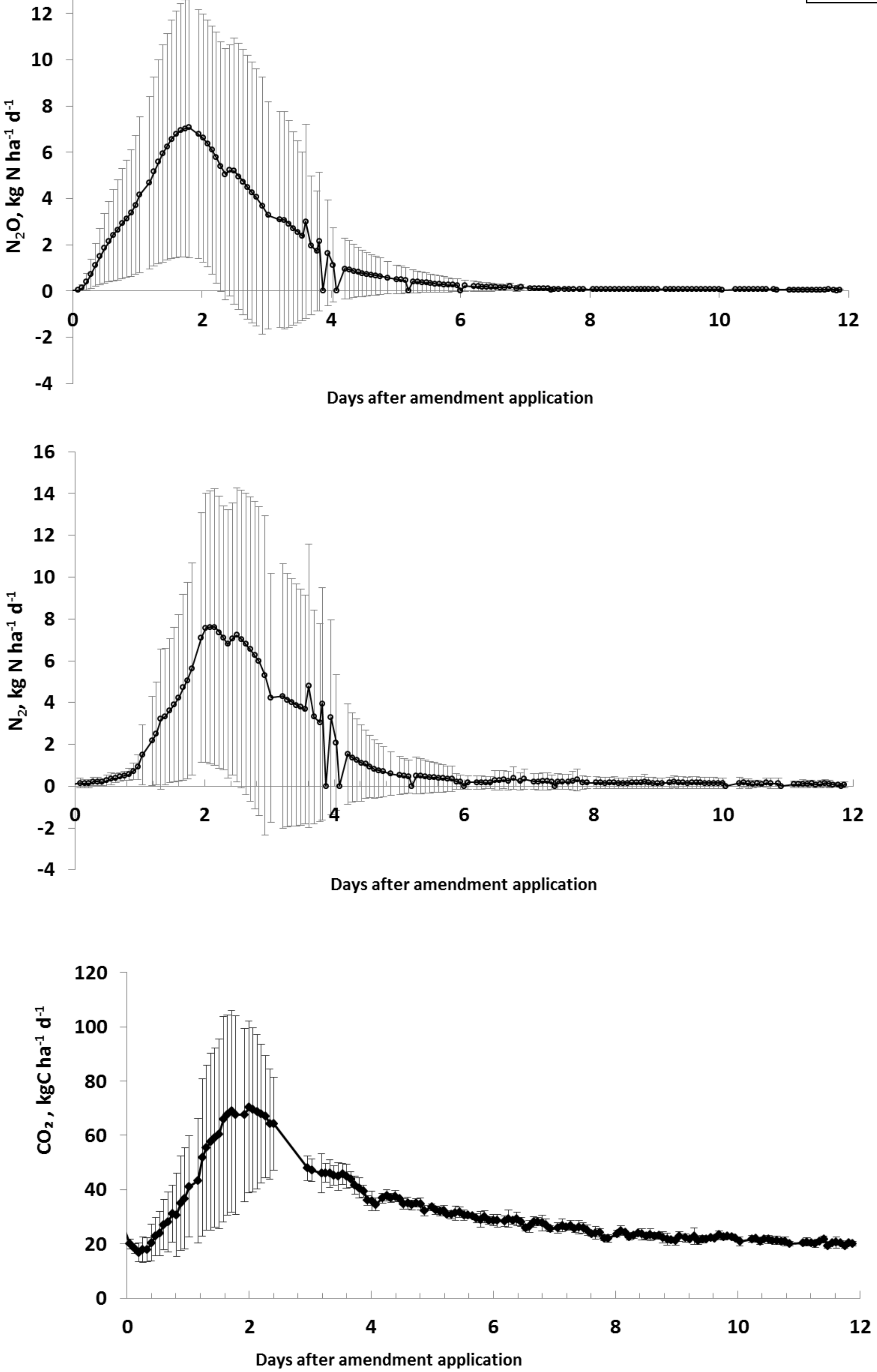

N2O, kg N ha-1 d-1
Days after amendment application
N2, kg N ha-1 d-1
Days after amendment application
CO2 , kgC ha-1 d-1
Days after amendment application

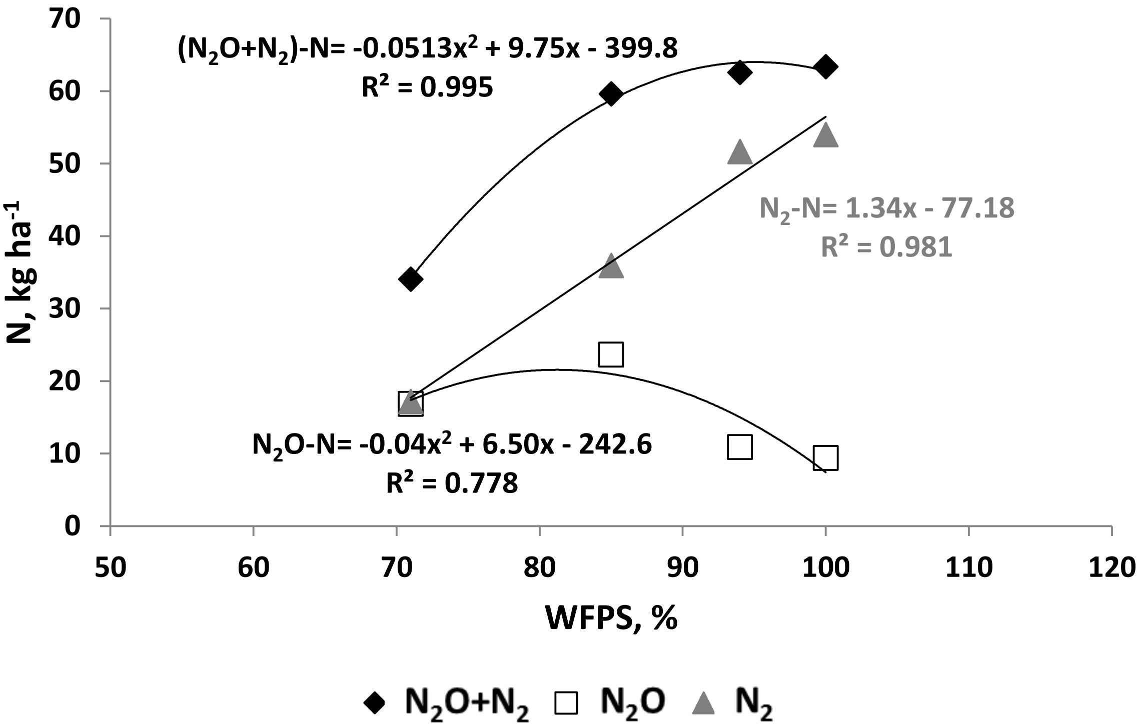
(N2O+N2)-N= -0.0513x2 + 9.75x - 399.8
R² = 0.995
N2-N= 1.34x - 77.18
R² = 0.981
N2O-N= -0.04x2 + 6.50x - 242.6
R² = 0.778
N, kg ha-1
WFPS, %
0
10
20
30
40
50
60
70
50
60
70
80
90
100
110
120
N2O+N2
N2O
N2

Figure 2

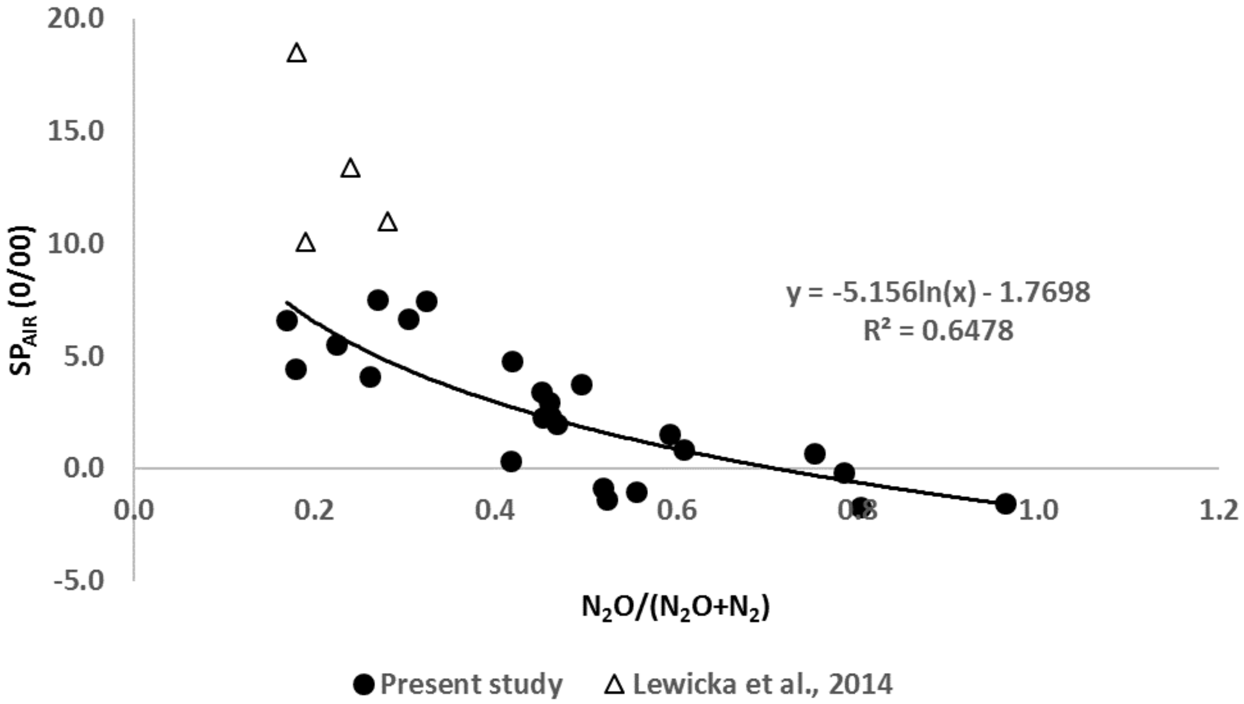
20.0
15.0
10.0
5.0
0.0
-5.0
0.0
0.2
0.4
0.6
0.8
1.0
1.2
SP_{AIR} (0/00)
$N_2O/(N_2O+N_2)$
y = -5.156ln(x) - 1.7698
$R^2 = 0.6478$
Present study
Lewicka et al., 2014

Figure 3

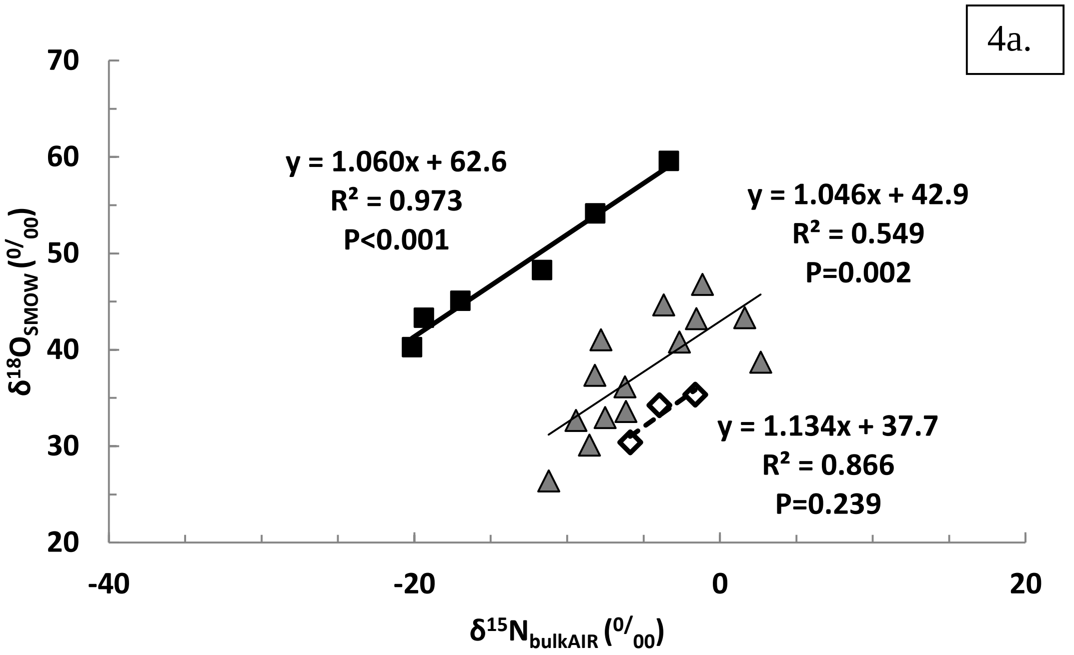
4a.
y = 1.060x + 62.6
R² = 0.973
P<0.001
y = 1.046x + 42.9
R² = 0.549
P=0.002
y = 1.134x + 37.7
R² = 0.866
P=0.239
δ18OSMOW (0/00)
δ15NbulkAIR (0/00)
70
60
50
40
30
20
-40
-20
0
20

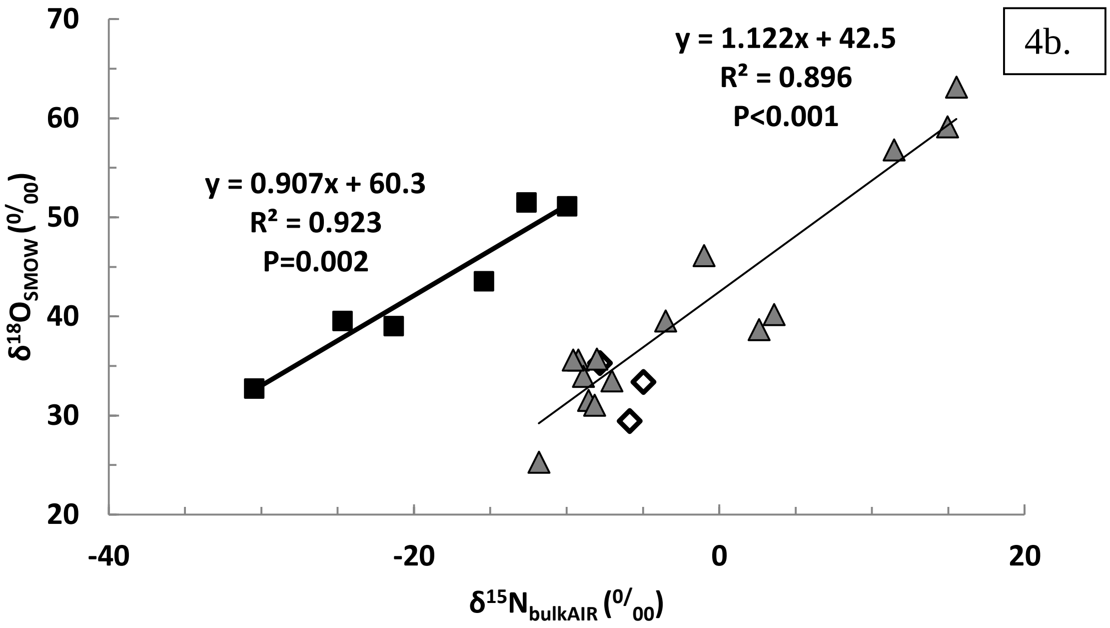
4b.
y = 1.122x + 42.5
R² = 0.896
P<0.001
y = 0.907x + 60.3
R² = 0.923
P=0.002
δ18OSMOW (0/00)
δ15NbulkAIR (0/00)
70
60
50
40
30
20
-40
-20
0
20

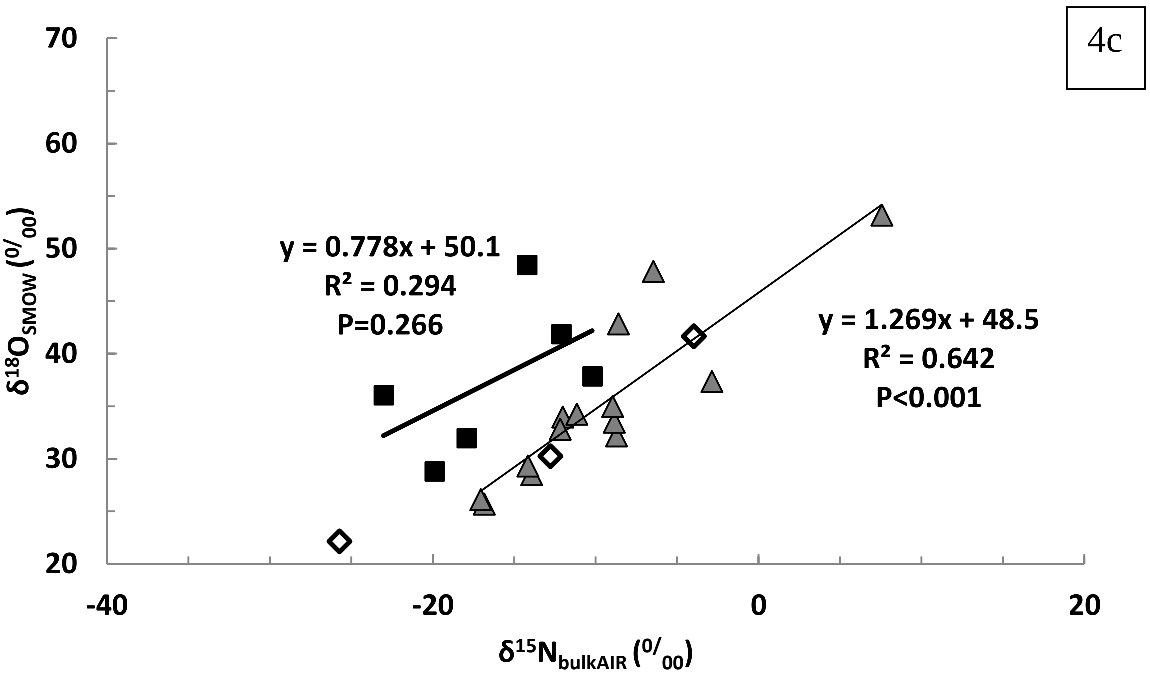
4c
70
60
50
40
30
20
-40
-20
0
20
$\delta^{18}O_{SMOW}$ ($^0/_{00}$)
$\delta^{15}N_{bulkAIR}$ ($^0/_{00}$)
y = 0.778x + 50.1
R² = 0.294
P=0.266
y = 1.269x + 48.5
R² = 0.642
P<0.001

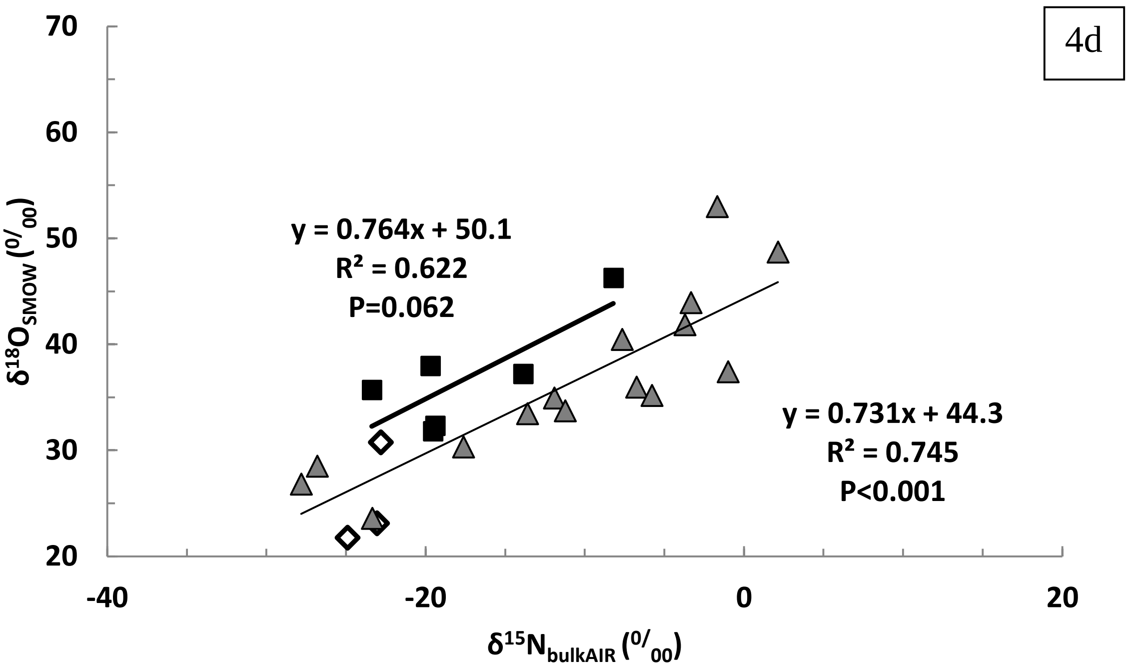
4d
70
60
50
40
30
20
-40
-20
0
20
$\delta^{18}O_{SMOW}$ ($^0/_{00}$)
$\delta^{15}N_{bulkAIR}$ ($^0/_{00}$)
y = 0.764x + 50.1
R² = 0.622
P=0.062
y = 0.731x + 44.3
R² = 0.745
P<0.001

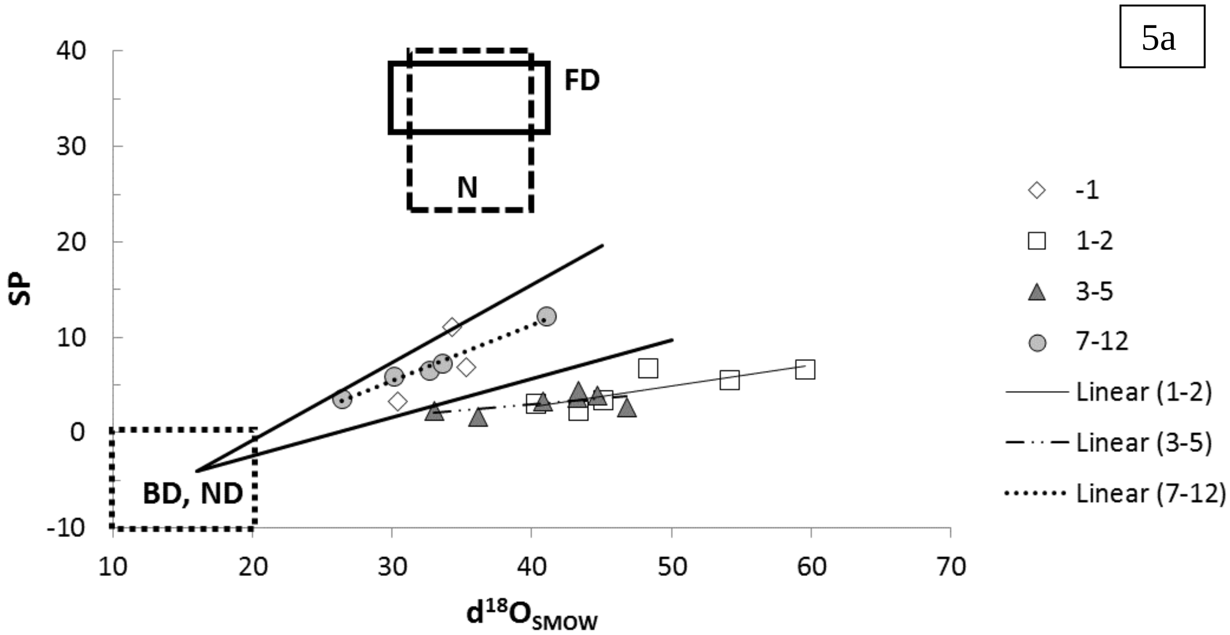
5a
SP
d18OSMOW
FD
N
BD, ND
-1
1-2
3-5
7-12
Linear (1-2)
Linear (3-5)
Linear (7-12)
40
30
20
10
0
-10
10
20
30
40
50
60
70

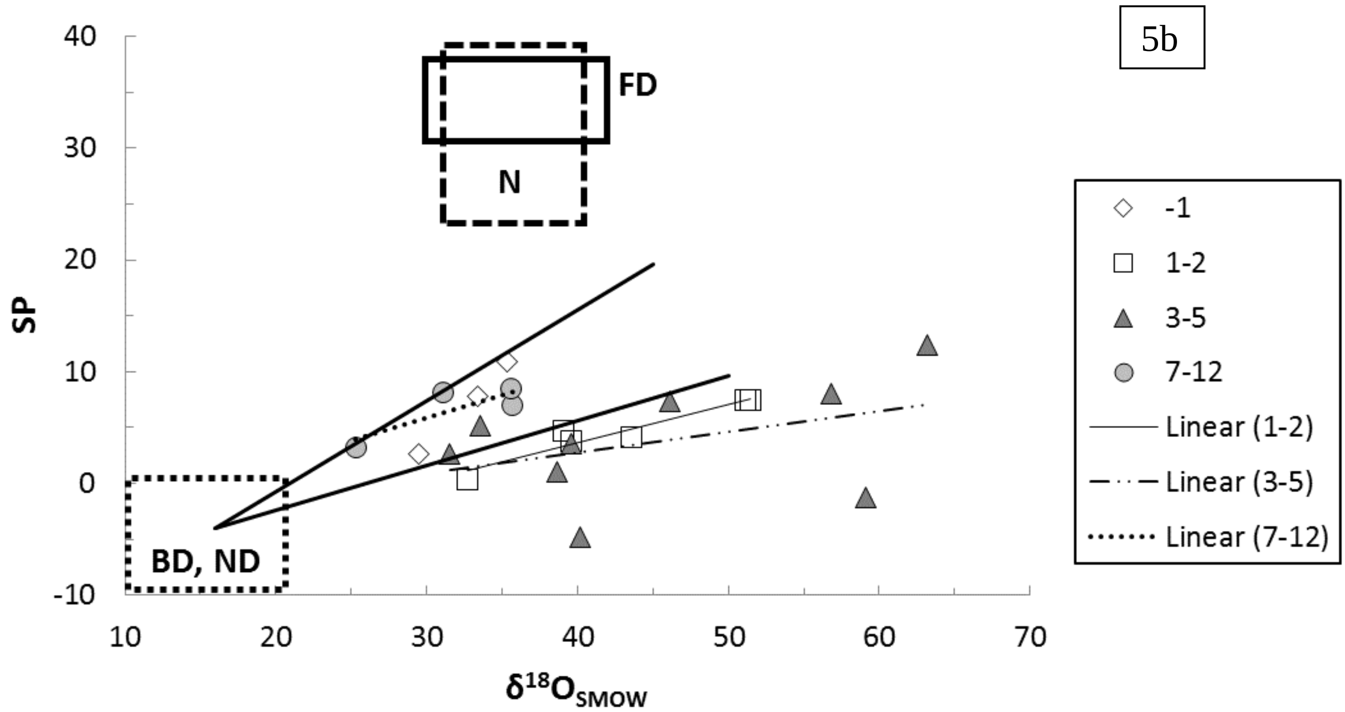
5b
SP
δ18OSMOW
FD
N
BD, ND
-1
1-2
3-5
7-12
Linear (1-2)
Linear (3-5)
Linear (7-12)
40
30
20
10
0
-10
10
20
30
40
50
60
70

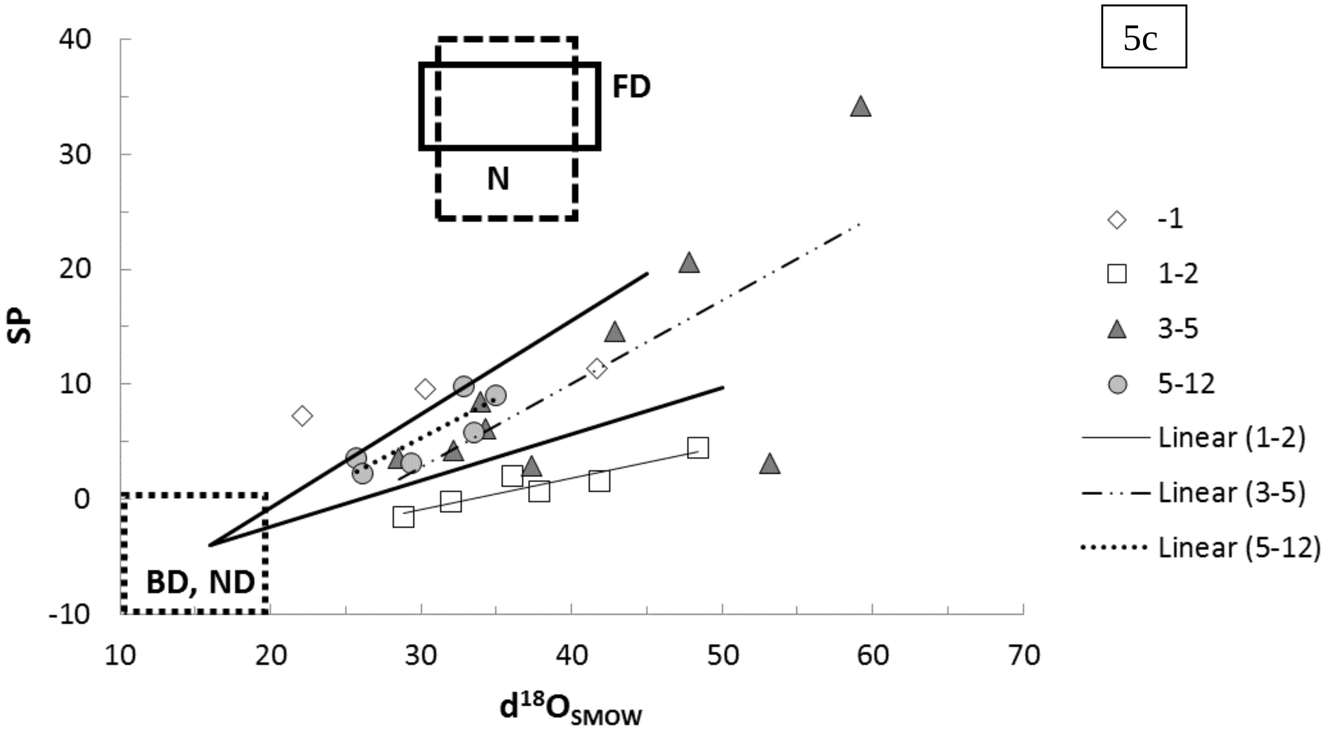
5c
FD
N
BD, ND
SP
d18OSMOW
-1
1-2
3-5
5-12
Linear (1-2)
Linear (3-5)
Linear (5-12)

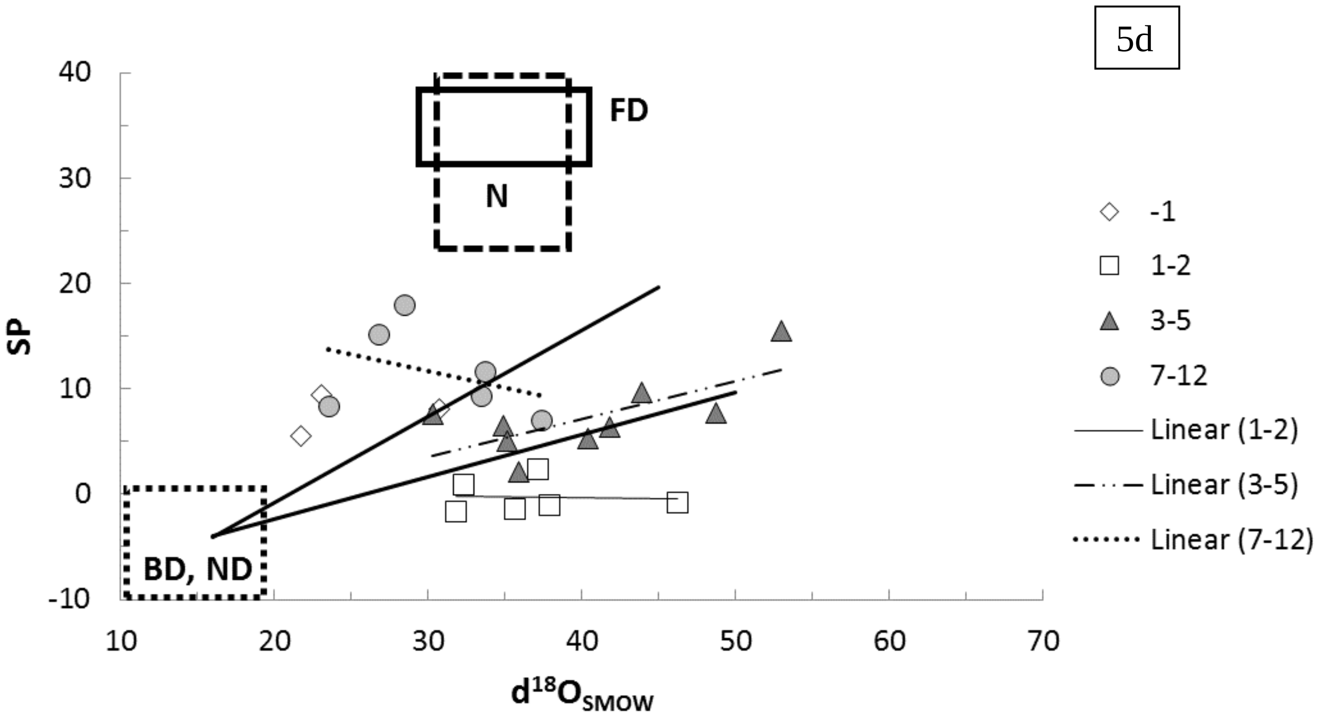
5d
FD
N
BD, ND
SP
d18OSMOW
-1
1-2
3-5
7-12
Linear (1-2)
Linear (3-5)
Linear (7-12)